Diacylglycerol acyltransferase 2 (DGAT2) links glucose utilization to fatty acid oxidation in the brown adipocytes

Zehra Irshad, Frederica Dimitri, Mark Christian and Victor A Zammit[1]

Division of Biomedical Sciences

Warwick Medical School, CV4 7AL, UK

[1]Corresponding author: Email: v.a.zammit@warwick.ac.uk

Fax: +44 (0)2476522798

Short title: DGAT2 enables BAT thermogenesis from glucose

Abbreviations:

Astat: Atglistatin

Etmox: Etomoxir

DGAT1-iB: DGAT1-specific inhibitor (cis-4-{3-fluoro-4-[({5-[(4-fluorophenyl)amino]-1,3,4-oxadiazol-2-yl}; carbonyl)-amino]phenoxy} cyclohexane carboxylic acid)

DGAT2-iC: DGAT2-selective inhibitor (N-(4,5-dihydronaphthol[1.2-d]thiazol-2-yl)-2-(3,4-dimethoxyphenyl)acetamide)

DAGT2-iJ: DGAT2- specific inhibitor (3-bromo-4-[2-fluoro-4-({4-oxo-2-[(2-pyridin-2-ylethyl)amino]1,3-thiazol-5(4H)-ylidene} methyl)phenoxy] benzonitrile)

Key words

From JLR list:

Adipocytes; DGAT; Fatty acid/Metabolism; Lipolysis; Adipose tissue

Additional key words:

Thermogenesis; *de novo* lipogenesis; β3-agonist; substrate channelling; brown adipose tissue.

SUMMARY

Brown adipose tissue uptake of glucose and fatty acids is very high during non-shivering thermogenesis. Adrenergic stimulation markedly increases glucose uptake, *de novo* lipogenesis and FA oxidation simultaneously. The mechanism that enables this concerted response has hitherto been unknown. Here we find that in a brown adipocyte cell line (IMBAT-1) acute inhibition and longer-term knockdown of DGAT2 links the increased *de novo* synthesis of fatty acids from glucose to a pool of TG which is simultaneously hydrolysed, providing FA for mitochondrial oxidation. DGAT1 does not contribute to this pathway, but uses exogenous FA and glycerol to synthesise a pool of TG from which the labelling of CO_2 is very low; DGAT2 also contributes to it. The DGAT2-dependent channelling of ^{14}C from glucose into TG and CO_2 was reproduced in β3-agonist-stimulated primary brown adipocytes. Knockdown of DGAT2 in IMBAT-1 affected the mRNA levels of several genes important in FA activation and esterification. Therefore, in β3-agonist activated brown adipocytes, DGAT2 specifically enables channelling of *de novo* synthesised FA into a rapidly mobilised pool of TG which is simultaneously hydrolysed to provide substrates for mitochondrial fatty acid oxidation.

INTRODUCTION

The diacylglycerol acytransferases, DGAT1 and DGAT2 catalyse the last, dedicated step of triacylglercerol (TG) synthesis. Although they catalyse the same reaction (with minor differences in substrate preferences) and are co-expressed in all the cell types in which they occur, they are functionally non-redundant. In particular, in the liver, DGAT2 is specialised for the formation of TG from *de novo* synthesised fatty acids and newly formed diglycerides (DG) thus acting upstream of DGAT1 in the *de novo* synthesis of TG (1). This renders DGAT2 essentially rate-limiting for the *de novo* formation of TG in the liver (2), and is consistent with the observation that the liver of mice lacking a key enzyme of the glycerol-3-P pathway (*Gpat 1*$^{-/-}$) is depleted of TG, and is unable to esterify *de novo* synthesised FA to TG (3). Although DGAT2 also participates in the maintenance of the TG pool(s) in lipid droplets through the lipolysis-reesterification cycling that occurs between TG and DG (4), the esterification between preformed FA and partial glycerides is primarily performed by DGAT1 in HepG2 cells (1) and in murine liver (5). This is consistent with the observations that *Dgat 1*$^{-/-}$ and *Dgat 2*$^{-/-}$ mice have very different phenotypes, with *Dgat 1*$^{-/-}$ animals having a metabolically favourable phenotype (including lower plasma and tissue TG) (6), whereas *Dgat 2*$^{-/-}$ animals dying within several hours after birth, and being devoid of TG (lipopenic) (7). This specialisation of hepatic DGAT2 for the utilization of *de novo* synthesised fatty acids (FA) is readily rationalised in view of the role of the liver in integrating glycaemia, triglyceridaemia and hepatic TG content, and accommodating large fluxes of glucose metabolism, *de novo* lipogenesis (DNL) and TG synthesis/secretion that it accommodates (2). However, the wider applicability, to other tissues and conditions, of this functional specialization of DGAT2 remains to be determined (8,9).

Brown adipose tissue (BAT) is another tissue that, like the liver, clears large amounts of both glucose and FA (either non-esterified or as products of lipoprotein lipase action on triglyceride-rich lipoproteins) from the circulation (10). The very high rates of uptake have been suggested to play a role in the regulation of glycaemia and triglyceridaemia (11-13). During cold exposure, BAT has the highest rate of glucose uptake and lipogenesis when compared to white adipose tissue (WAT) and the liver (14). BAT glucose metabolism is independent of insulin but, during β-adrenergic stimulation,

is stimulated by an increase in GLUT1 expression (via cAMP) and translocation to the plasma membrane, mediated through mTORC2 (15,16). Although glucose makes a relatively minor *direct* contribution (<20%) towards thermogenesis (through glycolysis and oxidation of pyruvate) (17,18), the contribution through oxidation of FA synthesised *de novo* from glucose and other lipogenic substrates (e.g. lactate (19)) could be considerably larger (13) . Indeed, when non-shivering thermogenesis is maximally stimulated, BAT can account for 33% of whole-body lipogenesis, and newly synthesised FAs make a significant contribution towards the thermogenic capacity of BAT in adult rodents (14). The very substantial lipogenic capacity of BAT (20) and its activation *in vivo* upon cold-exposure of animals (21,22) are accompanied by increased nuclear expression of SREBP1 and elevated gene expression of lipogenic and FA-elongation enzymes when mice are maintained at sub-thermoneutral temperatures (23).

Therefore, in view of the very high lipogenic potential of BAT (10,24,25), the contribution of *de novo* synthesised FA towards BAT thermogenesis may be substantial (13,26). FA, whether provided exogenously or synthesised *de novo* from glucose, activate UCP1 (by over-riding the inhibitory action of purine nucleotides on the protein), and provide the ultimate substrate for uncoupled respiration in brown adipocytes (27). Glucose is also required to form glycerol-3-P for the (re)synthesis of TG from FA. Therefore, like the liver, BAT has to integrate large fluxes of glucose and fatty acid metabolism, and may be a tissue in which the distinctive functions of DGAT1 and DGAT2 may be important in directing different FA pools towards specific pathways during adrenergic stimulation, when glucose uptake, *de novo* lipogenesis (DNL) and TG lipolysis are all coordinately activated (21,22,28). Expression profiling of mouse tissues, indicates that DGAT2 is expressed in BAT judging by the high level of its mRNA expressed in the tissue (29) and that its expression is increased (more than that of DGAT1) in BAT of cold-acclimated rodents (30). Therefore, in the present study, we have investigated the roles of DGAT1 and DGAT2 in the metabolism of glucose and *de novo* synthesised FA, compared to that of exogenous fatty acids in a brown adipocyte cell line (IMBAT-1) and in mouse primary brown adipocytes. We identified a specific role for DGAT2 in linking glucose uptake and DNL to the formation of TG which acts directlyde novo as a source of FA for oxidation, independently from the uptake and metabolism of extracellular FA.

MATERIALS AND METHODS

Preparation and culture of primary brown adipocytes

Mouse primary brown adipocytes were prepared from the stromal fraction resulting from the collagenase digestion of inter-scapular brown adipose tissue obtained from 4-week old mice. The stromal fraction was suspended in DMEM10, filtered through a 40µm strainer, and cells plated in T25 flasks. The cells were allowed to expand until 80-90% confluent with regular replacement of media. After trypsinization and resuspension in DMEM10 medium 5 x 10^4cells/well of 12-well plate were then plated and allowed to reach 100% confluence. Differentiation was induced by addition of medium containing insulin (1µg/ml), IBMX (250uM), triiodothyronine, T3 (1nM), indomethacin (30µM), rosiglitazone (2µM) and dexamethasone (0.5µM). After 96h, during which the medium was replenished once, the cells were switched to maintenance medium (DMEM10 medium supplemented with insulin, T3 and rosiglitazone only). After a further 48h, the cells were switched to a medium which contained the same concentrations of insulin and T3, but from which rosiglitazone was omitted. After a further 48h the medium was changed to DMEM10, and the cells were used for experimental treatments.

Generation, differentiation and culture of IMBAT-1 cells

The immortalised brown adipocyte cell line (IMBAT-1) was generated as described previously (31). Briefly, preadipocytes isolated from murine interscapular brown adipose tissue were immortalized by retroviral-mediated expression of temperature-sensitive SV40 large T-antigen H-2kb-tsA58. Cells were cultured in DMEM-F12 medium (20mM D glucose) supplemented with 10% foetal bovine serum (FBS), 1% L-glutamine, 1% Penicillin/streptomycin, Amphotericin B and 50µg/ml of G418 at 33°C in 5% CO_2 and 95% air- water saturated atmosphere. Unless specified otherwise, cells were passaged and harvested after treatment with 0.25% trypsin and 0.02% EDTA. For differentiation to mature adipocytes, pre-adipocytes were plated onto gelatine-coated plates and cultured until confluent. Induction medium containing 7.5mM glucose, 1µg/ml insulin, 250nM dexamethasone, 0.5mM IBMX, 1nM triidothyronine (T3) and 125µM Indomethacin was added for 48 hours at 37°C. Cells were then maintained in 7.5mM glucose medium containing 1nM T3 and 1µg insulin /ml for 5 days at 37°C. Unless

otherwise stated, all experiments were performed on day 7 of differentiation or after a further 72h treatment with siRNA. The experimental incubation medium was DMEM-F12 medium containing 7.5mM D-glucose, 10% fetal bovine serum, 1% L-glutamine, 1% penicillin/streptomycin, 1mM L-carnitine, 0.75mM oleate with 0.25% BSA and 0.75mM glycerol.

SiRNA-mediated knockdown of DGAT1 or DGAT2

Transfections were carried out on the day 7 of differentiation using Smartpool siRNA, designed by the manufacturers for DGAT1 and DGAT2, and transfection reagent lipofectamine RNAiMax, following the manufacturer's instructions. Differentiated adipocytes were dissociated with trypsin/EDTA followed by addition of DMEM/F12 with 10% FBS. Mixtures of transfection reagents, OptiMEM medium, 10μM siRNA-DGAT1 or 10μM siRNA-DGAT2 or 10μM siRNA-control were incubated at room temperature for 25 min. They were then added to the dissociated cells along with antibiotic-free DMEM-F12 medium (7.5mM glucose). Control cells were treated with scrambled siRNA. Media were changed after 24 hours and cells were cultured for further 48 hours at 37°C in maintenance medium. Preliminary experiments established that optimal knockdowns were achieved after 72h of siRNA treatment.

Measurement of the incorporation of ^{14}C-glucose label into CO_2 and cellular TG

IMBAT-1 or primary brown adipocytes cells plated in gelatine-coated 6-well plates containing 7.5mM glucose medium were incubated for 2h in the presence or absence of the β3-adrenergic agonist CL (10μM) before the addition of label to start the measurements. Preliminary experiments established the incorporation of [U-^{14}C]-glucose into labelled products was linear for 2h and this period was used routinely when [U-^{14}C]-glucose incorporation was studied. Where indicated, oleate or palmitate (0.75mM plus 0.25% albumin) and glycerol (0.75mM) were added to the incubations. When incorporation of label from 1-[^{14}C]-oleate, U-[^{14}C]-palmitate or 2-[^{3}H]-glycerol was measured, the labelling period was 1h to ensure linearity of incorporation into TG. In one series of experiments labelling with exogenous 1-[^{14}C]-oleate was extended to 8h to monitor the release of $^{14}CO_2$. When effects of DGAT1 or DGAT2 inhibition were studied, the appropriate inhibitors were added 30 min before the start of the incubations with the label. Where indicated, etomoxir (80 μM) was added 30 min before the start of the

experimental period by addition U-^{14}C-glucose label. Lipolysis was inhibited by addition of tetrahydrolipstatin (THL, 200µM) or Atglistatin (10µM) at the same time as the addition of CL i.e. 2 hours before addition of U-^{14}C-glucose label.

Measurement of $^{14}CO_2$ labelling

Formation of $^{14}CO_2$ after incubation of cells with labelled substrates for the required period of time was measured by transferring 1 ml of the incubation medium to a 20-ml glass conical flask containing a 0.5-ml Fisher centre well holding filter paper to which 400µl of benzethonium hydroxide had been added (32). The flask was stoppered and 1.0 ml of 1 M H_2SO_4 was injected through the rubber stopper. The flasks were shaken for 60 min at 37°C to allow the liberated $^{14}CO_2$ to be absorbed by the benzethonium hydroxide, after which the radioactivity associated with the contents of the centre-well was quantified using a liquid scintillation counter.

Measurement of incorporation of label into TG

At the end of the incubation period, the cells were washed with cold PBS, and total lipids were extracted from them using a chloroform/methanol mixture (2:1 v/v) (33). The chloroform layer was aspirated into a glass tube and dried under a stream of N_2 gas. The dried material was re-solubilized in chloroform (500µl) and the entire volume was applied onto a TLC plate coated with Silica Gel 60 for separation of the radioactive triglyceride product, using hexane/diethyl ether/formic acid (70:30:1, v/v/v) as the mobile phase. A TG-standard (tripalmitin) was used to identify the position of the TG band visualized using iodine vapour. The radioactivity associated with each band was quantified after scraping into scintillation vials, addition of scintillant (Ultima Gold™, Perkin Elmer) and measuring the associated radioactivity using a scintillation counter.

Saponification of the total lipids was performed as described in (34) with minor modifications. The cellular total lipid extract were dried and dissolved in 0.75ml of 30% KOH and heated at 70°C for 10 min. An equal volume of 95% ethanol was then added and the mixture was heated at 70 °C for 2 hours. After cooling, the aqueous fraction was acidified with 3M HCl and extracted thrice with light petroleum. The organic fraction was evaporated, re-dissolved in 1ml of light petroleum, transferred to scintillation vial and quantified as the TG-acyl fraction. The remaining aqueous fraction contained the TG-

glyceryl fraction; 0.5ml aliquot of this sample was taken and measured for radioactivity using scintillation counter.

Real time PCR quantitation of mRNA expression

Total RNA was extracted from IMBAT-1 cells using TRIzol reagent. cDNA was prepared using reverse transcription. Briefly RNA (1ug) was mixed with oligodT (1µl) in a final volume of 12 µl by adding RNAse free water. Samples were heated at 70°C for 5 min before chilling on ice. Subsequently, 8µl of mixture containing RNAse inhibitor (10 U/µl), dNTPs (10 mM), Bioscript reverse transcriptase and RNAse free water were added to each sample. Samples were heated at 40 °C for 60 min and the reaction was stopped by heating to 70 °C for 10min. The cDNA formed was mixed with 180µl of nuclease-free water and stored at -20°C. Samples were thawed only once before quantification. Reverse transcription (RT-PCR) was performed using SYBR green dye and expression for all the samples ($n \geq 3$) was calculated by using the DCt method, incorporating the efficiencies of each primer pair. The variances of input cDNA were normalised against the levels of three housekeeping genes; L19, B-actin and 36B4. Melting curve analysis confirmed amplification specificity. The primers used are detailed in Table S1 of the supplementary material.

Statistical analyses

Differences between means for independent groups of data were analysed by ANOVA followed by the post hoc Tukey test.

Materials

Dulbecco's Modified Eagle's Medium DMEM10, DMEMF12, etomoxir sodium salt, CL, L-carnitine, benzethonium hydroxide, light petroleum (bp: 40-60 °C), glyceryl tripalmitate, sodium oleate, insulin, IBMX, Indomethacin, and 3,3'5-triiodo-L-thyamine were purchased from Sigma-Aldrich. TLC-pre-coated plates, 10ml conical flasks with centre wells, lipofectamine, and RNAiMax were purchased from Fischer scientific. Rosiglitazone was from Cayman Chemical. Radiolabelled [U-^{14}C]-glucose (specific activity 250-360mCi/mmol), [1-^{14}C] Oleic acid (specific activity: 40-60mCi/mmol) and [2-^{3}H] glycerol (specific activity 0.5-1.0 Ci/mmol) was purchased from Perkin Elmer LAS (UK). ON-TARGETplus Mouse Dgat1 smartpool siRNA, ON-TARGETplus Mouse Dgat2

smartpool siRNA and ON-TARGETplus non-targeting siRNA were purchased from GE Healthcare UK. Of the three inhibitors of DGAT activity used, *DGAT1iB* (cis-4-{3-fluoro-4-[({5-[(4-fluorophenyl)amino]-1,3,4-oxadiazol-2-yl}carbonyl)-amino]phenoxy} cyclohexane carboxylic acid) and *DGAT2-iC* (N-(4,5-dihydronaptht*h*ol[1.2-d]thiazol-2-yl)-2-(3,4-dimethoxyphenyl)acetamide) used were obtained from Astra Zeneca and have been used previously as DGAT1 and DGT2 inhibitors, respectively (33). A third inhibitor, DGAT2-i*J* (3-bromo-4-[2-fluoro-4-({4-oxo-2-[(2-pyridin-2-ylethyl)amino]1,3-thiazol-5(4H)-ylidene}methyl)phenoxy] benzonitrile) was obtained from Janssen Research and Development UK, and has been used previously as a specific DGAT2 inhibitor (5). All primers were purchased from Sigma-Aldrich.

RESULTS

A. Experiments using the brown adipocyte-derived cell line IMBAT-1

In view of the large amount of preliminary work that was needed to establish the conditions under which the metabolic fluxes of interest could be measured, and the concentrations of inhibitors required, we used a well-established brown adipocyte-derived cell line, IMBAT-1. This cell line has been well characterised, and has been shown to express all the proteins that are characteristic of brown adipocytes, especially UCP1 (35). Their use also allowed us to verify the effects observed with specific DGAT1 and DGAT2 inhibitors through the efficient knockdown of the two proteins in these cells using siRNA.

The main findings were validated using primary brown adipocytes (see below).

A.1 DGAT2 mRNA expression is preferentially induced during differentiation

We investigated the expression of DGATs across a panel of murine tissues. DGAT2 mRNA was most highly expressed in BAT, and present at much lower levels in WAT, liver, intestine and mammary gland (**Figure 1**). DGAT1 mRNA was most highly expressed in the intestine, followed by BAT, white adipose tissue and mammary gland. We then studied the profile of mRNA expression for both DGATs, compared with the differentiation marker aP2 during brown adipocyte differentiation. All three mRNAs were induced at day 2 of differentiation, but whereas DGAT1 mRNA was induced

moderately during the first days of differentiation, levelling off thereafter and declining on day 6, DGAT2 mRNA was induced 10-fold more strongly and continued to be induced throughout the period of differentiation, levelling off at day 6 (**Figure 2**). This time course of the expression of the two genes is the opposite to that previously described during the differentiation of white adipocytes, in which an initial peak in DGAT2 expression (during initial differentiation with glucose as the main substrate) is overtaken by a sustained expression of DGAT1 mRNA during the latter stages of differentiation (35).

A.2 β3-adrenergic stimulation increases incorporation of de novo synthesised FA into TG and CO_2

We next measured the rates of labelling from U-^{14}C-glucose into TG and CO_2 in IMBAT-1 cells, and ascertained that they were linear during the 2h-period of the incubations (not shown). Stimulation of IMBAT-1 cells with the β3-agonist CL316324 (CL) for 2h before the start of incubations (by addition of U-^{14}C-glucose label) resulted in a significant increase in the incorporation of ^{14}C-label from glucose into CO_2 (**Figure 3a**). The rates of CL-stimulated glucose incorporation were 22.8 ±1.3 and 50.6 ±1.0 pmol/h/10^6cells for TG-acyl and TG-glyceryl moieties, respectively. The incorporation into CO_2 was 10.6± 1.4 pmol/h/10^6cells, although this flux is not directly comparable to the previous two, as (i) $^{14}CO_2$ is generated both during lipogenesis and FA oxidation, and (ii) $^{14}CO_2$ derived from the oxidation of *de novo* synthesised FA will have been diluted by unlabelled acyl moieties within the pre-existing TG pool. From the observation that 10^6 cells yield approximately 10mg wet weight of cellular material, it is calculated that these rates are of the same order of magnitude as the values reported for glucose uptake (~7.2 μm/h/g) and *de novo* lipogenesis rates (~4.8 μm/h/g) in cold-acclimated rats *in vivo* (14,30).

Etomoxir (an inhibitor of CPT1 which controls FA entry into mitochondria (36)) inhibited CO_2 labelling marginally under basal conditions (**Figure 3**) suggesting that, as expected, in the absence of CL-stimulated TG lipolysis, CO_2 labelling from glucose was due mostly to that generated in the course of lipogenesis. The increase in CO_2 labelling induced by CL was totally prevented by etomoxir (**Figure 3a**). As a result, it could be calculated that CL increased the rate of $^{14}CO_2$ labelling due to CPT 1-dependent oxidation of *de novo* synthesised FA by approximately 4-fold (**Fig 3a**).

Stimulation of the cells with CL also activated incorporation of label from U-^{14}C-glucose into both parts of the TG molecule (glyceryl and acyl, **Figures 3b and 3c**, respectively) although differentially. Stimulation of U-^{14}C-glucose incorporation into the acyl moieties of the TG molecule was consistently significantly higher (2-fold) than that into the glyceryl moiety of TG (50%) indicating that, whereas increased glucose uptake by the cells by CL may have been a common contributor towards the increased labelling of TG from glucose (25), *de novo* lipogenesis was stimulated independently of, and to a higher extent than, the pathway leading from glucose to triose phosphates (the last common intermediates of glycerol-3-P and FA formation). Etomoxir did not affect incorporation of glucose into TG-acyl or TG-glyceryl moieties, confirming that its action is specific to the inhibition of FA oxidation.

A.3 CL-stimulation of glucose incorporation into TG-FA and their oxidation is ATGL-dependent

To test the possible role of TG synthesis and hydrolysis in the provision of glucose-derived FA for oxidation, we tested the effects of inhibition of TG hydrolysis, using Atglistatin (a specific inhibitor of adipose triglyceride lipase, ATGL) and the non-specific lipase inhibitor tetrahydrolipstatin (THL). Both inhibitors prevented all the effects of CL treatment on CO_2 and TG labelling from U-^{14}C-glucose without affecting basal rates (**Figure 4**). CL-stimulation of the incorporation of glucose into both acyl and glyceryl moieties of TG was totally prevented by ATGL. This indicated that a metabolite generated by TG lipolysis activates one or more steps in the pathways leading from glucose to TG synthesis, and occurs independently of the interruption of the provision of FA for oxidation as a result of the inhibition of TG hydrolysis. This positive feedback on TG synthesis supports previous observations that TG lipolysis generates signalling molecules that affect lipogenic fluxes (37-39).

A.4 Oxidation of de novo synthesised FA is DGAT2-dependent

In view of the preferential activation of the esterification of *de novo* synthesised FA into TAG labelled from glucose, we studied the possibility that DGAT1 and DGAT2 may have different roles in the esterification of newly synthesised FA into TG after β3-stimulation of IMBAT-1 cells. We used three compounds which have previously been

well-characterised as specific inhibitors of the two DGATs. Compound *DGAT1-iB* was previously used (1,33,40,41) as a highly specific inhibitor of DGAT1; Compound *DGAT2-iC* (see methods) was used in (1) as a selective inhibitor of DGAT2 at lower concentrations; and compound *DGAT2-iJ* was developed and used as a highly specific inhibitor of DGAT2 ((5); see Methods). As these compounds have been developed as inhibitors of the human enzymes, we performed dose-response studies to ascertain that they were effective inhibitors of TG synthesis in IMBAT-1 cells at concentrations that were not deleterious to cell viability. The concentrations required for each compound to inhibit incorporation of U-^{14}C-glucose into the glyceryl or acyl moieties of TG (not shown) were similar to those found to be effective in HepG2 cells and on the recombinant human enzymes (1,5,33). In the same experiments, we quantified cell viability, as judged by MTT mitochondrial viability assays, at the end of the 2h incubations. Thereafter, the effects of DGAT1 or DGAT2 inhibition were investigated in detail, using single concentrations of each compound (see Legends to Figures) that gave significant inhibitory effects but with the retention of full cell viability.

Both the DGAT2 inhibitors tested (*DGAT2-iC* and *DGAT2-iJ*) resulted in a strong inhibition of the CL-stimulated incorporation of ^{14}C-glucose into CO_2 and TG-acyl groups (see **Figure 5 a, b**). By contrast, inhibition of DGAT1 (with *DGAT1-iB*) did not affect either incorporation of label into $^{14}CO_2$ (**Fig 5a**) or into TG-acyl groups (**Fig 5b**). These observations suggest that DGAT2 activity is specialised for the esterification of *de novo* synthesised fatty acids into TG and subsequent mitochondrial oxidation of FA products of TG lipoloysis. The validity of this conclusion is strengthened by the demonstration of the ability of the two structurally unrelated inhibitors of DGAT2 to produce identical effects. Both DGAT1 and DGAT2 inhibition decreased significantly the glucose incorporation into the glyceride part of TG (**Fig 5c**), indicating that glycerol-3-P newly synthesised from glucose is incorporated into DG pools that are used by either DGAT1 or DGAT2 as substrates.

Importantly, the above observations were not altered qualitatively when experiments were conducted in the presence of added exogenous glycerol (0.75mM) and oleate (0.75mM in the presence of 0.25% albumin) to the medium **(Figure 5d-f)**;only DGAT2 inhibition resulted in the loss of labelling from U-^{14}C-glucose into TG-acyl moieties and CO_2 (**Figure 5d, e**). Therefore, addition of exogenous oleate (or palmitate, not shown) did not affect the ability of DGAT2 inhibition specifically to affect the

incorporation of *de novo* synthesised FA into TG (compare **Figure 5b** and **5e**) or the formation of CO_2 after CL treatment. These observations indicate that *de novo* synthesised FA are compartmentalised rapidly into a pool of TG which is not accessible to exogenously added FA. Addition of exogenous glycerol and oleate appeared to increase the effect of either DAGT1 or DGAT2 inhibition on glucose incorporation into TG-glyceryl, but did not affect the relative importance of the two enzymes in this process (compare **Figure 5c and f**).

To exclude the possibility that non-specific effects of enzyme inhibitors were compromising the validity of our observations, we investigated the longer-term effects of the knockdown of the expression of either protein using individually targeted siRNA treatment of IMBAT-1 cells. The effects of 72h siRNA treatment on mRNA expression of the DGAT1 and DGAT2 are shown in **Figure 6**. A scrambled sequence was used in control cells. Note that reliable quantification of protein expression was not possible using a range of commercially available antibodies (not shown). Similarly, DGAT activities could not be reliably quantified by available DGAT assays using the amounts of material available.

The data in **Figure 7a** show that knockdown of DGAT2 had a major inhibitory effect on the incorporation of label from U-^{14}C-glucose into CO_2 both under basal and CL-stimulated conditions, indicating that *de novo* synthesised FA need to be incorporated into TG by DGAT2 before they can undergo mitochondrial oxidation in IMBAT-1 cells. Importantly, knockdown of DGAT1 did not have this effect at all (**Figure 7a**). Therefore, these data are identical qualitatively and quantitatively to those obtained using the respective DGAT1 and DGAT2 inhibitors (**Figure 5**). Knockdown of DGAT2 also had a large inhibitory effect on the incorporation of glucose into TG (**Figure 7b**). Saponification of the lipid fraction confirmed the preferential stimulus of glucose incorporation into the acyl moieties of TG, and showed that DGAT2 knockdown had large inhibitor effects on the incorporation of label from U-^{14}C-glucose into both TG-acyl and TG-glyceryl moieties under both basal and CL-stimulated conditions (**Figure 7e, f**). Therefore, effects of longer-term DGAT2 down-regulation with siRNA treatment on the formation of TG-acyl moieties, and their subsequent use for $^{14}CO_2$ were quantitatively similar to those observed after short-term inhibition (**Figure 5**). By contrast, there was no effect on glucose incorporation onto TG-acyl when DGAT1 was knocked down (**Figure 7d**), and much smaller effects than those achieved by DGAT2 knockdown on

incorporation of glucose into TG-glyceryl (**Figure 7c**). These observations confirm that DGAT2 is specialised for the channelling of *de novo* synthesised fatty acids towards oxidation (to CO_2) initially through their incorporation into a distinct pool of TG, followed by lipolysis.

DGAT1 knockdown was completely ineffective in altering ^{14}C-glucose incorporation into TG-acyl, and had a smaller effect on incorporation into TG-glyceryl moieties than that observed after DGAT2 knockdown. Therefore, these data provide evidence that, in cells subjected to longer-term downregulation of either DGAT isoform, endogenously synthesised glycerol-3-P is preferentially used, to a considerable extent, to synthesise a distinct pool of DG that acts as a substrate for DGAT2 (compare **Figures 7c** and **7e**).

A.5 DGAT2 knockdown attenuates the CL-mediated induction of UCP1 mRNA expression

In view of the observed close association between DGAT2 down-regulation and metabolism of *de novo* synthesised FA, we investigated whether long-term down-regulation of DGAT2 or DGAT1 is accompanied by changes of lipogenic gene expression. We measured the mRNA expression (before and after CL treatment) of UCP1 and of several genes which are involved in the pathways leading from glucose to TG synthesis and CO_2 formation (**Figure 8**). Incubation of the cells with CL for 2h increased the expression of UCP1 mRNA four-fold in IMBAT-1 cells (as observed previously in BAT *in vivo* (42)); DGAT2 knockdown resulted in the halving of this increase whereas DGAT1 knockdown had no effect (**Figure 8**). CL-treatment also resulted in a significant induction of the mRNA expression of GPAT1; downregulation of either DGAT1 or DGAT2 increased basal expression of GPAT1 mRNA, whereas there was no effect of DGAT1 knockdown on GPAT4 expression. By contrast, both GPAT4 and Elvol6 mRNA expressions were decreased specifically by DGAT2 siRNA treatment both under basal and CL-stimulated conditions. None of the other genes tested (including Elvol3, not shown) showed significant differences in mRNA expression levels after CL-stimulation or knockdown of either DGAT compared to control (scrambled) siRNA-treated cells.

Therefore, knockdown of DGAT2 moderately but specifically affected the expression of three genes that are central to elongation of *de novo* synthesised FA (Elvol6), FA

esterification (GPAT4), and uncoupling of mitochondrial FA oxidation (UCP1) (3,43,44) indicating that it may play a central role in the maintenance of BAT function.

A.6 Direct oxidation of exogenously added oleate is very low

We next compared the roles of DGAT1 and DGAT2 in determining the metabolism of exogenously added, preformed fatty acids. We performed a series of experiments in which the normal concentration of unlabelled glucose was accompanied by glycerol (0.75 mM) and oleate (0.75 mM in the presence of 0.25% albumin). We performed parallel experiments in which we labelled either the glycerol (2-^{3}H-glycerol) or oleate (1-^{14}C-oleate). We also used U-^{14}C-palmitate to verify that the effects observed with oleate could be replicated using a saturated FA; the results with palmitate (not shown) were identical to those obtained with oleate.

Contrary to the incorporation of *de novo* synthesised FA and glycerol-3-P derived from U-^{14}C-glucose, the labelling of TG from either exogenous glycerol or oleate were not stimulated by CL, showing that the effects of the β3-agonist were specific to the stimulation of glucose metabolism and FA derived from it. Although exogenous 1-^{14}C-oleate was very rapidly incorporated into TG (75 ± 9 nmol oleate/h/10^{6} cells), no significant ^{14}C-label above background was recovered in oxidation products (either CO_2 or acid-soluble metabolites, ASM). Thus, although we used specific activities of 1-^{14}C-oleate (and U-^{14}C-palmitate) to provide the same degree of overall cellular TG labelling as that achieved by U-^{14}C-glucose, only minimal ^{14}C-label was recovered in CO_2 or ASM after exposure to 1-^{14}C-oleate even when incubations were extended to 8h after addition of label to eliminate the possibility of a time-lag (not shown). There are two conclusions from these observations. Firstly, that exogenous FA are not oxidised directly to CO_2 to any significant extent in IMBAT-1 cells, although they are rapidly incorporated into TG. Secondly, that the pool of TG into which exogenous oleate is esterified is distinct from that into which *de novo* synthesised FAs are esterified by DGAT2, since the latter do give rise to $^{14}CO_2$ linearly over a 2h incubation period. This is consistent with the observation in ***A.4***, above, that addition of exogenous oleate did not alter the pattern of fluxes of U-[^{14}C]-glucose into TG-acyl or TG-glyceryl moieties. The simplest explanation for these combined observations is that exogenous (pre-formed) oleate is incorporated into a separate, large pool of TG in which the specific activity of 1-^{14}C-oleate is highly diluted, resulting in a low specific activity of TG-acyl groups, and thus in negligible labelling of the

CO_2 produced from the oxidation of its constituent FA after lipolysis. *De novo* synthesised fatty acids, which labelled total cellular TG to the same extent, appear to have been incorporated into a TG pool in which a much higher specific activity of the acyl groups was achieved, before their oxidation $^{14}CO_2$ (which could be easily quantified). Therefore, this pool must be considerably smaller, and must turn over rapidly to give the linear and immediate CO_2 formation observed.

These inferences were supported by the effects on exogenous 1-^{14}C-oleate incorporation into TG after the inhibition of either DGAT1 (using *DGAT1-iB*) or DGAT2 (using *DGAT2-iJ*). When added individually, each inhibitor affected only marginally the incorporation of exogenous 1-^{14}C-oleate into TG. However, incubation of cells simultaneously with both *DGAT1-iB* and *DGAT2-iJ* resulted in almost complete inhibition of labelling of TG from exogenously added 1-^{14}C-oleate (**Figure 9a**)**.** Therefore, the esterification of FA derived from exogenous, pre-formed oleate (or palmitate, not shown) can be catalysed redundantly by either DGAT1 or DGAT2. Only the combined inhibition of the two enzymes decreased esterification of exogenously added oleate into TG significantly (**Figure 9a**). This was entirely different from the ability of DGAT2 down-regulation specifically to inhibit TG-acyl labelling from glucose.

Incorporation of 2-[^{3}H]-glycerol into TG was maximally decreased by inhibition of DGAT1 (**Figure 9b**). Although DGAT2 inhibition also moderately decreased 2-^{3}H-glycerol incorporation into TG, this effect was much smaller than that of DGAT1 inhibition, and combined DGAT2 and DGAT1 inhibition did not increase that achieved by DGAT1 inhibition alone. Therefore, exogenous glycerol is used for the synthesis of DG which serves preferentially as a substrate for DGAT1 (**Figure 9b**), whereas glucose-derived glycerol-3-P is used preferentially for the synthesis of DG used by DGAT2 (**Figure 7e**).

B. Experiments using mouse primary brown adipocytes

Having established the experimental conditions for the use of DGAT1 and DGAT2 inhibitors, we wanted to validate the salient aspects of our observations using mouse primary brown adipocytes. This enabled us to ascertain that the same conclusions are applicable in a cell system closer to the physiological condition.

B.1 CL stimulates etomoxir-sensitive glucose incorporation into CO_2

When primary brown adipocytes were treated with CL, the rate of CO_2 formation from U-^{14}C-glucose was increased by 5.5-fold (**Fig 10**). This was prevented by etomoxir, indicating that the glucose had to be converted into FA before it was oxidised. This inference was confirmed by the demonstration that incubation with TOFA (an inhibitor of lipogenesis at the ATP-citrate lyase step) also inhibited the etomoxir-sensitive incorporation of glucose into CO_2 (**Figure 10**). Although this scale of activation was similar to the 4-fold stimulation by CL of etomoxir-sensitive conversion of glucose into CO_2 observed in IMBAT-1 cells (see above), it occurred over a much lower background of CO_2 production in control primary cells. The absolute rates of incorporation of U-^{14}C-glucose into CO_2, TG-acyl and TG-glyceryl were 15.1 ± 1.1, 10.0 ± 1.5 and 10.0 ± 2.1 nmol/h/10^6 cells, respectively. Therefore, primary brown adipocytes had very similar rates of glucose incorporation as IMBAT-1 cells (see above) but were more oxidative over the experimental period used (1 -2 h), suggesting that the mobilization of the TG pool feeding into oxidation is even more rapid than in IMBAT-1 cells. Consequently, β3-adrenergic stimulation of the flux of glucose into CO_2 and its prevention by inhibition of DGAT2 (see below) was more pronounced in primary cells.

B.2 Inhibition of DGAT2 but not of DAGT1 prevents incorporation of U-^{14}C from glucose into TG

Glucose incorporation into TG-acyl and TG-glyceryl moieties were both prevented by DGAT2 inhibition in primary brown adipocytes (**Figure 10 a, b**). Moreover, this effect was mimicked by the inhibition of *de novo* FA synthesis with TOFA (an inhibitor of *de novo* lipogenesis) indicating that DGAT2 utilises newly synthesised diglycerides and FA to form a distinct pool of TG. Inhibition of DGAT1 had no effect whatever on incorporation of labelled glucose into TG-acyl groups (as observed in IMBAT-1 cells). Although there was a tendency for the inhibition of DGAT1 to affect incorporation into TG-glyceryl groups the effect was less than that shown by DGAT2 inhibition (as in IMABT-1 cells), and did not reach statistical significance (**Figure 10 a**).

B.3 Inhibition of DGAT2, but not DGAT1, prevents glucose conversion into CO_2

The CL-induced increase in CO_2 production from glucose was entirely prevented by inhibition of DGAT2 (**Figure 10c**), confirming that, as in IMBAT-1 cells, the FA

synthesised from glucose had to be incorporated into TG before they could be oxidised (subsequent to lipolysis). By contrast, inhibition of DGAT1 had no effect on the etomoxir-sensitive conversion of glucose into CO_2. Therefore, the data obtained with primary brown adipocytes fully confirmed our IMBAT-1 observations on the specialised role of DGAT2 in channelling *de novo* synthesised FAs towards oxidation in brown adipocytes. The effect of DGAT2 was mimicked by inhibition of CPT1 with etomoxir and by the inhibition of *de novo* lipogenesis by TOFA (**Figure 10c**) confirming that DGAT2 action lies on a pathway linking DNL to FA oxidation in brown adipocytes.

Discussion

Glucose is one of the two major substrates used by BAT. The high rate of glucose uptake during cold exposure acts as a 'glucose sink' able to improve insulin sensitivity physiologically during cold exposure (9,45) and after pharmacological activation aimed at increasing glucose utilization by BAT to regulate blood glucose in obesity and diabetes (12,45,46). Although BAT bioenergetics are centred around the uncoupled oxidation of FA as the source of thermogenic capacity, there is a strong relationship between FA oxidation and glucose uptake in BAT (47); glucose-derived pyruvate makes only a minor *direct* contribution towards mitochondrial electron transport chain activity. The simultaneous activation of glucose transport, *de novo* fatty acid synthesis and fatty acid oxidation (FAO) in brown adipocytes by β-adrenergic stimulation (14,48,49) is consistent with the observations of increased expression of enzymes involved in FA-synthesis (e.g. FSN), FA-desaturation (SCD1) and FA–elongation (e.g. Elvol3, Elvol6) after cold-exposure or CL-treatment *in vivo* (13,23,37). However, the rationale for the oxidation of newly synthesised FA has previously been questioned and considered paradoxical (9,10). It has been proposed that the newly synthesised FA are not oxidised immediately, but are stored in LDs in anticipation of subsequent thermogenic activation (10,24,30).

The present study has addressed this apparent paradox by showing that, in the brown adipocytes (primary cells and IMBAT-1 cell line), glucose-derived FAs are specifically channelled into a rapidly mobilised pool of TG, which is distinct from the bulk TG pool into which exogenous, preformed FA are esterified. This is evidenced by the DGAT2-dependence of the labelling of CO_2 derived from *de novo* synthesised FA, but not that derived from exogenous oleate, in spite of equivalent overall labelling of total cellular TG by both substrates. The ability of TOFA (an inhibitor of FA synthesis) to replicate the

effects of DGAT2 inhibition supports the concept that channelling of *de novo* synthesised FA towards oxidation occurs via DGAT2-mediated TG synthesis. This segregation of a glucose-derived, DGAT2-dependent synthesis of a distinct pool of TG enables the cell to oxidise *de novo* synthesised FA directly, and independently from FA derived exogenously. Therefore, DGAT2 acts as the link between increased glucose utilization and uncoupled mitochondrial FA oxidation, as part of a concerted response of this pathway to adrenergic stimulation in brown adipocytes (see **Figure 11**). Previous experiments performed *in vivo* had found evidence for distinct pools of TG being used to channel FAs towards oxidation or esterification (50,51) and for the dependence of the stereospecific distribution ion cellular TG of *de novo* synthesised and exogenous FA (52,53). The current observations on the specialisation of TG formed via DGAT1 or DGAT2 provide a mechanism through which these distinct TG pools could be achieved.

When we tested this concept in primary brown adipocytes, we found that in this cellular model too, DGAT2 (but not DGAT1) inhibition totally prevented incorporation of glucose into TG acyl and TG-glyceryl moieties, and the formation of CO_2 from *de novo* synthesised FA. Indeed, because primary brown adipocytes are more oxidative than IMBAT-1 cells, the role of DGAT2 in mediating the channelling of glucose carbons towards FA oxidation was even more apparent. Moreover, we demonstrated that the effect of DGAT2 inhibition on these parameters could be mimicked by inhibition of *de novo* lipogenesis with TOFA, thus showing the close link between DGAT2 action and utilization of *de novo* synthesised FAs for TG synthesis and subsequent oxidation.

The specialised role of DGAT2 in esterifying *de novo* synthesised FAs is similar to that described originally in HepG2 cells (1,2). More recently, urokinase-type Plasminogen Activator (uPA) has been shown to stimulate TG synthesis from acetate, in parallel with increased *de novo* lipogenesis (DNL) and the specific induction of the expression of DGAT2 (54). These observations suggest that this specialised function of DGAT2 may be a ubiquitous function of this enzyme in different cell types, with metabolic outcomes depending on tissue function, e.g. linking glycaemia to triglyceridaemia in the liver (2), and the channelling of glucose-derived FA towards rapid oxidation in BAT (present data).

The ability of ATGL inhibition to prevent the CL-mediated stimulation of CO_2 formation from *de novo* synthesised FA derived from glucose would be expected to result from the interruption of FA supply by inhibition of TG lipolysis. However, in addition,

ATGL inhibition also prevented the stimulation of glucose incorporation into TG (both glyceride and acyl moieties) indicating that a product of lipolysis activates glucose metabolism by the cells through a positive feedback mechanism (**Figure 10**). Inhibition of TG lipolysis is suggested to have interrupted this feedback activation of one or more steps leading from glucose to the synthesis of glycerol-3-P, *de novo* FA synthesis and esterification into TG. This is consistent with previous observations that in *Atgl* $^{-/-}$ mice BAT shows diminished glucose uptake (55), and that ATGL expression is essential for β3-activation of DNL in BAT *in vivo* (37,55). Our data suggest that in IMBAT-1 cells DNL is stimulated to a greater extent than incorporation of glucose-derived glyceryl moieties into TG; therefore, positive feedback activation of DNL may occur partly independently of triose-phosphate formation. The importance of ATGL in the provision of ligands for the positive feedback-activation of PPARα target gene activation is well-established (56).

A proportion of the CO_2 labelling from U-^{14}C-glucose arises during decarboxylation of pyruvate and the direct oxidation of the resulting acetyl-CoA through the TCA cycle; this is known to make only a minor contribution towards thermogenesis (19). We distinguished between this direct oxidation of glucose and the CO_2 derived from FA oxidation by using etomoxir. This inhibitor of CPT1 decreased CO_2 labelling only moderately in the absence of CL, but totally prevented the stimulation (4-fold in IMBAT-1 cells and 5.5-fold in primary adipocytes) mediated by CL indicating that the increased formation of $^{14}CO_2$ from glucose after CL stimulation was entirely due to increased oxidation of *de novo* synthesised FA.. Importantly, the CL-mediated and etomoxir-sensitive stimulation of CO_2 labelling from glucose was specifically prevented by down-regulation of DGAT2, but not of DGAT1. This indicated that (i) DNL and TG synthesis precede the formation of CO_2, and (ii) that DGAT2 is specifically involved in this pathway. Such sensitivity to DGAT2 down-regulation reinforces the conclusion that CO_2 production does not occur directly from the *de novo* synthesised FAs, but only subsequent to TG formation. Oxidation of exogenously added fatty acids is deduced to have been similarly indirect in IMBAT-1 cells because detection of labelled CO_2 or acid-soluble metabolite (ASM) formation was very low when cells were incubated with 1-^{14}C-oleate or U-^{14}C-palmitate, in spite of their very rapid labelling of cellular TG. This was also the case in primary cells (not shown). As mentioned above, this can be explained if the added ^{14}C-oleate was esterified into a large, pre-existing pool of TG within which its specific activity

was highly diluted. This indirect route for FA oxidation has been described for several tissues and cell types (57-60).

It is evident that the specialisation of DGAT2 action for the esterification of *de novo* synthesised FA and nascent DG containing these FA provides a mechanism for channelling glucose-derived FAs towards uncoupled FA oxidation upon adrenergic stimulation. It is well-established that the activation of ATGL by β3-adrenergic agonism promotes TG turnover by simultaneously promoting glucose uptake and DNL, including the induction of proteins involved in DNL (37), thus providing substrates for DGAT2. Because of the importance of long-chain acyl-CoA synthase 1 (ACSL1) in channelling FA (whether supplied exogenously or synthesised *de novo*) towards mitochondrial β-oxidation and of GPAT4 in diverting FA towards TG synthesis (27,61), we considered whether the very low rates of labelling of $^{14}CO_2$ from exogenously added 1-^{14}C-oleate to generate directly could have been due to a low expression of ACSL1 from IMBAT-1 cells. This possibility was excluded because we detected high levels of expression of ACSL1 mRNA (**Figure 8**). In addition, adequate expression of ACSL1 can also be inferred from the observation that *de novo* synthesised FA were oxidised rapidly to CO_2 simultaneously with TG labelling from glucose in a DGAT2-dependent manner. Both GPAT1 and GPAT4 expressions were partly dependent on DGAT2 expression in IMBAT-1 cells (**Figure 8b**), and may play a major role in ensuring that both endogenously derived and exogenously added FA are esterified to TG prior to oxidation.

In IMBAT-1 cells, DGAT1 and DGAT2 act redundantly for the incorporation of glucose-derived glycerol-3-P into TG, although less so after longer-term knockdown. However, exogenous glycerol is used preferentially for the formation of DG utilised by DGAT1, indicating that the two enzymes also have differential access to DG synthesised from exogenous or endogenously synthesised glycerol-3-P. This compartmentalization is different from the observations previously made on two liver systems (HepG2 cells (1) and murine liver (5)) in which DGAT2 is specialised for the incorporation of exogenous glycerol into TG. This difference in the handling of glycerol-3-P formed from exogenous glycerol may reflect the differences between the metabolism of TG in liver and BAT. Thus, lipolysis in BAT goes to completion (to glycerol and FA) whereas it is mostly restricted to the formation of DG and monoglyceride (MG) in the liver, e.g. in rat liver *in vivo* (62,63) and in primary rat hepatocytes (64). Therefore, in BAT, the lipolysis-reesterification cycling occurs between TG and FA, whereas in the liver cycling occurs

primarily between DG and TG, or MG and DG (64) without the release of glycerol. In the liver, DG is mostly used for the resynthesis of TG either for maintenance of cytosolic TG stores in lipid droplets, or incorporated into VLDL (1,2,65). The specialization of specific enzyme isoforms for the channelling of FA is increasingly being recognised (see (61,66)).

In summary, all our data on primary brown adipocytes and a brown adipocyte derived cell line indicate that the DGAT2-dependent pool of TG is distinct from that into which exogenous, preformed FA are esterified. As a result, newly synthesised FA are made immediately available for mitochondrial oxidation in a DGAT2-dependent manner. By contrast, exogenous FA are esterified into a separate, larger, pre-existing pool of TG. Assuming that this pool of TG is itself mobilised during β-adrenergic stimulation, this indicates that exogenous FA and *de novo* synthesised FA are esterified into separate TG pools before being oxidised. However, whereas DGAT2 is exclusively responsible for the formation of the TG pool specific for *de novo* synthesised FA, it also participates, together with DGAT1, in the (re)esterification of exogenous FA into the larger pool of cellular TG. These data suggest that within the multilocular structure of BAT lipid droplets, a sub-population of droplets, originate specifically as a result of DGAT2 activity, enriched in *de novo* synthesised FA, and preferentially mobilised to enable glucose to contribute immediately towards thermogenesis. This is consistent with the previous observation that, within a given cell, individual lipid droplets have differential access to the TG biosynthetic machinery (67).

The very high level of expression of DGAT2 mRNA in the tissue *in vivo*, and its large fold-induction and persistence during IMBAT-1 cell differentiation are indicative of the importance of DGAT2 expression for BAT function. In this context, the 4-fold induction of UCP1 in IMBAT-1 cells upon CL-stimulation is markedly blunted after knockdown of DGAT2 expression, suggesting that DGAT2 expression is important for the maintenance of the brown adipocyte phenotype. It is noteworthy that *Dgat2*$^{-/-}$ mice do not survive beyond 12h after birth. This has been ascribed to defects in skin lipid synthesis, and the associated dehydration (7). Our data raise the possibility that they may also be unable to thermoregulate normally. It is well-established that deficient thermogenesis results in increased mortality in neonatal rodents (68) and that prevention of glucose uptake by BAT *in vivo* by down-regulation of mTORC2 results in hypothermia (16). Although it is likely that the contribution that glucose makes towards heat production in BAT is not fully developed in the neonate (owing to the lower rates of DNL in the tissue before

weaning (14)) it would become more important as the pups switch to a high carbohydrate diet (at 2 – 3 weeks of age) such that glucose- and DGAT2-dependent non-shivering thermogenesis post-weaning might become critical for survival. Moreover, the role of DGAT2 in enabling glucose utilization for BAT thermogenesis (and possible glycaemic and body weight control) needs to be considered when developing pharmacological strategies aimed at using the modulation of BAT activation to control glycaemia and triglyceridaemia in obesity and diabetes.

ACKNOWLEDGEMENTS

This work was supported by a Medical Research Council UK grant to VAZ. The authors thank Jensen and AstraZeneca and Jensen for the provision of inhibitor compounds.

REFERENCES

1. Wurie, H. R., Buckett, L., and Zammit, V. A. (2012) Diacylglycerol acyltransferase 2 acts upstream of diacylglycerol acyltransferase 1 and utilizes nascent diglycerides and de novo synthesized fatty acids in HepG2 cells. *FEBS J* **279**, 3033-3047

2. Zammit, V. (2013) Hepatic Triglyceride Synthesis and Secretion:DGAT2 as the Link between Glycaemia and Triglyceridaemia. *Biochemical Journal* **451**, 1 - 12

3. Wendel, A. A., Cooper, D. E., Ilkayeva, O. R., Muoio, D. M., and Coleman, R. A. (2013) Glycerol-3-phosphate acyltransferase (GPAT)-1, but not GPAT4, incorporates newly synthesized fatty acids into triacylglycerol and diminishes fatty acid oxidation. *J Biol Chem* **288**, 27299-27306

4. Eichmann, T. O., Kumari, M., Haas, J. T., Farese, R. V., Jr., Zimmermann, R., Lass, A., and Zechner, R. (2012) Studies on the substrate and stereo/regioselectivity of adipose triglyceride lipase, hormone-sensitive lipase, and diacylglycerol-O-acyltransferases. *J Biol Chem* **287**, 41446-41457

5. Qi, J., Lang, W., Geisler, J. G., Wang, P., Petrounia, I., Mai, S., Smith, C., Askari, H., Struble, G. T., Williams, R., Bhanot, S., Monia, B. P., Bayoumy, S., Grant, E., Caldwell, G. W., Todd, M. J., Liang, Y., Gaul, M. D., Demarest, K. T., and Connelly, M. A. (2012) The use of stable isotope-labeled glycerol and oleic acid to differentiate the hepatic functions of DGAT1 and -2. *J Lipid Res* **53**, 1106-1116

6. Chen, H. C., Smith, S. J., Ladha, Z., Jensen, D. R., Ferreira, L. D., Pulawa, L. K., McGuire, J. G., Pitas, R. E., Eckel, R. H., and Farese, R. V., Jr. (2002) Increased insulin and leptin sensitivity in mice lacking acyl CoA:diacylglycerol acyltransferase 1. *J Clin Invest* **109**, 1049-1055.

7. Cases, S., Stone, S., Zhou, P., Yen, E., Tow, B., Lardizabal, K. D., Voelker, T., and Farese, R. V., Jr. (2001) Cloning of DGAT2, a second mammalian diacylglycerol acyltransferase, and related family members. *J. Biol. Chem.* **276**, 38870-38876

8. Li, C., Li, L., Lian, J., Watts, R., Nelson, R., Goodwin, B., and Lehner, R. (2015) Roles of Acyl-CoA:Diacylglycerol Acyltransferases 1 and 2 in Triacylglycerol Synthesis and Secretion in Primary Hepatocytes. *Arterioscler Thromb Vasc Biol* **35**, 1080-1091

9. Townsend, K. L., and Tseng, Y. H. (2014) Brown fat fuel utilization and thermogenesis. *Trends Endocrinol Metab* **25**, 168-177

10. Cannon, B., and Nedergaard, J. (2004) Brown adipose tissue: function and physiological significance. *Physiol Rev* **84**, 277-359

11. Villarroya, F., and Vidal-Puig, A. (2013) Beyond the sympathetic tone: the new brown fat activators. *Cell Metab* **17**, 638-643

12. Whittle, A. J., Lopez, M., and Vidal-Puig, A. (2011) Using brown adipose tissue to treat obesity - the central issue. *Trends Mol Med* **17**, 405-411

13. Hankir, M. K., Cowley, M. A., and Fenske, W. K. (2016) A BAT-Centric Approach to the Treatment of Diabetes: Turn on the Brain. *Cell Metab* **24**, 31-40

14. Trayhurn, P. (1981) Fatty acid synthesis in mouse brown adipose tissue. The influence of environmental temperature on the proportion of whole-body fatty acid synthesis in brown adipose tissue and the liver. *Biochim Biophys Acta* **664**, 549-560

15. Olsen, J. M., Sato, M., Dallner, O. S., Sandstrom, A. L., Pisani, D. F., Chambard, J. C., Amri, E. Z., Hutchinson, D. S., and Bengtsson, T. (2014) Glucose uptake in brown fat cells is dependent on mTOR complex 2-promoted GLUT1 translocation. *J Cell Biol* **207**, 365-374

16. Albert, V., Svensson, K., Shimobayashi, M., Colombi, M., Munoz, S., Jimenez, V., Handschin, C., Bosch, F., and Hall, M. N. (2016) mTORC2 sustains thermogenesis via Akt-induced glucose uptake and glycolysis in brown adipose tissue. *EMBO Mol Med* **8**, 232-246

17. Saggerson, E. D., McAllister, T. W., and Baht, H. S. (1988) Lipogenesis in rat brown adipocytes. Effects of insulin and noradrenaline, contributions from glucose and lactate as precursors and comparisons with white adipocytes. *Biochem J* **251**, 701-709

18. Ma, S. W., and Foster, D. O. (1986) Uptake of glucose and release of fatty acids and glycerol by rat brown adipose tissue in vivo. *Can J Physiol Pharmacol* **64**, 609-614

19. Brito, M. N., Brito, N. A., Brito, S. R., Moura, M. A., Kawashita, N. H., Kettelhut, I. C., and Migliorini, R. H. (1999) Brown adipose tissue triacylglycerol synthesis in rats adapted to a high-protein, carbohydrate-free diet. *Am J Physiol* **276**, R1003-1009

20. Cooney, G. J., and Newsholme, E. A. (1982) The maximum capacity of glycolysis in brown adipose tissue and its relationship to control of the blood glucose concentration. *FEBS Lett* **148**, 198-200

21. Minokoshi, Y., Saito, M., and Shimazu, T. (1988) Sympathetic activation of lipid synthesis in brown adipose tissue in the rat. *J Physiol* **398**, 361-370

22. Yu, X. X., Lewin, D. A., Forrest, W., and Adams, S. H. (2002) Cold elicits the simultaneous induction of fatty acid synthesis and beta-oxidation in murine brown adipose tissue: prediction from differential gene expression and confirmation in vivo. *FASEB J* **16**, 155-168

23. Tan, Chong Y., Virtue, S., Bidault, G., Dale, M., Hagen, R., Griffin, Julian L., and Vidal-Puig, A. (2015) Brown Adipose Tissue Thermogenic Capacity Is Regulated by Elovl6. *Cell Reports* **13**, 2039-2047

24. Festuccia, W. T., Blanchard, P. G., Turcotte, V., Laplante, M., Sariahmetoglu, M., Brindley, D. N., Richard, D., and Deshaies, Y. (2009) The PPARgamma agonist rosiglitazone enhances rat brown adipose tissue lipogenesis from glucose without altering glucose uptake. *Am J Physiol Regul Integr Comp Physiol* **296**, R1327-1335

25. Orava, J., Nuutila, P., Lidell, M. E., Oikonen, V., Noponen, T., Viljanen, T., Scheinin, M., Taittonen, M., Niemi, T., Enerback, S., and Virtanen, K. A. (2011) Different metabolic responses of human brown adipose tissue to activation by cold and insulin. *Cell Metab* **14**, 272-279

26. Isler, D., Hill, H. P., and Meier, M. K. (1987) Glucose metabolism in isolated brown adipocytes under beta-adrenergic stimulation. Quantitative contribution of glucose to total thermogenesis. *Biochem J* **245**, 789-793

27. Ellis, J. M., Li, L. O., Wu, P. C., Koves, T. R., Ilkayeva, O., Stevens, R. D., Watkins, S. M., Muoio, D. M., and Coleman, R. A. (2010) Adipose acyl-CoA synthetase-1 directs fatty acids toward beta-oxidation and is required for cold thermogenesis. *Cell Metab* **12**, 53-64

28. Moura, M. A., Festuccia, W. T., Kawashita, N. H., Garofalo, M. A., Brito, S. R., Kettelhut, I. C., and Migliorini, R. H. (2005) Brown adipose tissue glyceroneogenesis is activated in rats exposed to cold. *Pflugers Arch* **449**, 463-469

29. Wu, C., Orozco, C., Boyer, J., Leglise, M., Goodale, J., Batalov, S., Hodge, C. L., Haase, J., Janes, J., Huss, J. W., 3rd, and Su, A. I. (2009) BioGPS: an extensible and customizable portal for querying and organizing gene annotation resources. *Genome Biol* **10**, R130

30. Labbe, S. M., Caron, A., Bakan, I., Laplante, M., Carpentier, A. C., Lecomte, R., and Richard, D. (2015) In vivo measurement of energy substrate contribution to cold-induced brown adipose tissue thermogenesis. *FASEB J* **29**, 2046-2058

31. Rosell, M., Kaforou, M., Frontini, A., Okolo, A., Chan, Y. W., Nikolopoulou, E., Millership, S., Fenech, M. E., MacIntyre, D., Turner, J. O., Moore, J. D., Blackburn, E., Gullick, W. J., Cinti, S., Montana, G., Parker, M. G., and Christian, M. (2014) Brown and white adipose tissues: intrinsic differences in gene expression and response to cold exposure in mice. *Am J Physiol Endocrinol Metab* **306**, E945-964

32. Hulver, M. W., Berggren, J. R., Cortright, R. N., Dudek, R. W., Thompson, R. P., Pories, W. J., MacDonald, K. G., Cline, G. W., Shulman, G. I., Dohm, G. L., and Houmard, J. A. (2003) Skeletal muscle lipid metabolism with obesity. *Am J Physiol Endocrinol Metab* **284**, E741-747

33. Wurie, H. R., Buckett, L., and Zammit, V. A. (2011) Evidence that diacylglycerol acyltransferase 1 (DGAT1) has dual membrane topology in the endoplasmic reticulum of HepG2 cells. *J Biol Chem* **286**, 36238-36247

34. Saggerson, E. D., and Greenbaum, A. L. (1970) The regulation of triglyceride synthesis and fatty acid synthesis in rat epididymal adipose tissue. *Biochem J* **119**, 193-219

35. Payne, V. A., Au, W. S., Gray, S. L., Nora, E. D., Rahman, S. M., Sanders, R., Hadaschik, D., Friedman, J. E., O'Rahilly, S., and Rochford, J. J. (2007) Sequential regulation of diacylglycerol acyltransferase 2 expression by CAAT/enhancer-binding protein beta (C/EBPbeta) and C/EBPalpha during adipogenesis. *J Biol Chem* **282**, 21005-21014

36. Zammit, V. A. (1999) The malonyl-CoA-long-chain acyl-CoA axis in the maintenance of mammalian cell function. *Biochem J* **343**, 505-515

37. Mottillo, E. P., Balasubramanian, P., Lee, Y. H., Weng, C., Kershaw, E. E., and Granneman, J. G. (2014) Coupling of lipolysis and de novo lipogenesis in brown, beige, and white adipose tissues during chronic beta3-adrenergic receptor activation. *J Lipid Res* **55**, 2276-2286

38. Haemmerle, G., Moustafa, T., Woelkart, G., Buttner, S., Schmidt, A., van de Weijer, T., Hesselink, M., Jaeger, D., Kienesberger, P. C., Zierler, K., Schreiber, R., Eichmann, T., Kolb, D., Kotzbeck, P., Schweiger, M., Kumari, M., Eder, S., Schoiswohl, G., Wongsiriroj, N., Pollak, N. M., Radner, F. P., Preiss-Landl, K., Kolbe, T., Rulicke, T., Pieske, B., Trauner, M., Lass, A., Zimmermann, R., Hoefler, G., Cinti, S., Kershaw, E. E., Schrauwen, P., Madeo, F., Mayer, B., and Zechner, R. (2011) ATGL-mediated fat catabolism regulates cardiac mitochondrial function via PPAR-alpha and PGC-1. *Nat Med* **17**, 1076-1085

39. Tang, T., Abbott, M. J., Ahmadian, M., Lopes, A. B., Wang, Y., and Sul, H. S. (2013) Desnutrin/ATGL activates PPARdelta to promote mitochondrial function for insulin secretion in islet beta cells. *Cell Metab* **18**, 883-895

40. Camus, G., Herker, E., Modi, A. A., Haas, J. T., Ramage, H. R., Farese, R. V., Jr., and Ott, M. (2013) Diacylglycerol acyltransferase-1 localizes hepatitis C virus NS5A protein to lipid droplets and enhances NS5A interaction with the viral capsid core. *J Biol Chem* **288**, 9915-9923

41. Herker, E., Harris, C., Hernandez, C., Carpentier, A., Kaehlcke, K., Rosenberg, A. R., Farese, R. V., Jr., and Ott, M. (2010) Efficient hepatitis C virus particle formation requires diacylglycerol acyltransferase-1. *Nat Med* **16**, 1295-1298

42. Mottillo, E. P., Bloch, A. E., Leff, T., and Granneman, J. G. (2012) Lipolytic products activate peroxisome proliferator-activated receptor (PPAR) alpha and delta in brown adipocytes to match fatty acid oxidation with supply. *J Biol Chem* **287**, 25038-25048

43. Tan, C. Y., Virtue, S., Bidault, G., Dale, M., Hagen, R., Griffin, J. L., and Vidal-Puig, A. (2015) Brown Adipose Tissue Thermogenic Capacity Is Regulated by Elovl6. *Cell Rep* **13**, 2039-2047

44. Yamashita, A., Hayashi, Y., Matsumoto, N., Nemoto-Sasaki, Y., Oka, S., Tanikawa, T., and Sugiura, T. (2014) Glycerophosphate/Acylglycerophosphate acyltransferases. *Biology (Basel)* **3**, 801-830

45. Stanford, K. I., Middelbeek, R. J., Townsend, K. L., An, D., Nygaard, E. B., Hitchcox, K. M., Markan, K. R., Nakano, K., Hirshman, M. F., Tseng, Y. H., and Goodyear, L. J. (2013) Brown adipose tissue regulates glucose homeostasis and insulin sensitivity. *J Clin Invest* **123**, 215-223

46. Bartelt, A., Bruns, O. T., Reimer, R., Hohenberg, H., Ittrich, H., Peldschus, K., Kaul, M. G., Tromsdorf, U. I., Weller, H., Waurisch, C., Eychmuller, A., Gordts, P. L., Rinninger, F., Bruegelmann, K., Freund, B., Nielsen, P., Merkel, M., and Heeren, J. (2011) Brown adipose tissue activity controls triglyceride clearance. *Nat Med* **17**, 200-205

47. Marette, A., and Bukowiecki, L. J. (1991) Noradrenaline stimulates glucose transport in rat brown adipocytes by activating thermogenesis. Evidence that fatty acid activation of mitochondrial respiration enhances glucose transport. *Biochem J* **277 (Pt 1)**, 119-124

48. Yu, Y. H., Zhang, Y., Oelkers, P., Sturley, S. L., Rader, D. J., and Ginsberg, H. N. (2002) Posttranscriptional control of the expression and function of diacylglycerol acyltransferase-1 in mouse adipocytes. *J Biol Chem* **277**, 50876-50884

49. Knight, B. L., Hebbachi, A., Hauton, D., Brown, A. M., Wiggins, D., Patel, D. D., and Gibbons, G. F. (2005) A role for PPARalpha in the control of SREBP activity and lipid synthesis in the liver. *Biochem J* **389**, 413-421

50. Banke, N. H., Wende, A. R., Leone, T. C., O'Donnell, J. M., Abel, E. D., Kelly, D. P., and Lewandowski, E. D. (2010) Preferential oxidation of triacylglyceride-derived fatty acids in heart is augmented by the nuclear receptor PPARalpha. *Circ Res* **107**, 233-241

51. Bu, S. Y., and Mashek, D. G. (2010) Hepatic long-chain acyl-CoA synthetase 5 mediates fatty acid channeling between anabolic and catabolic pathways. *J Lipid Res* **51**, 3270-3280

52. Henderson, R. J., Christie, W. W., and Moore, J. H. (1979) Positional distribution of exogenous and endogenous fatty acids in triacylglycerols formed by rat adipocytes in vitro. *Biochim Biophys Acta* **574**, 8-17

53. Henderson, R. J., Christie, W. W., and Moore, J. H. (1979) Esterification of exogenous and endogenous fatty acids by rat adipocytes in vitro. *Biochim Biophys Acta* **573**, 12-22

54. Paland, N., Gamliel-Lazarovich, A., Coleman, R., and Fuhrman, B. (2014) Urokinase-type plasminogen activator (uPA) stimulates triglyceride synthesis in Huh7 hepatoma cells via p38-dependent upregulation of DGAT2. *Atherosclerosis* **237**, 200-207

55. Hoy, A. J., Bruce, C. R., Turpin, S. M., Morris, A. J., Febbraio, M. A., and Watt, M. J. (2011) Adipose triglyceride lipase-null mice are resistant to high-fat diet-induced insulin resistance despite reduced energy expenditure and ectopic lipid accumulation. *Endocrinology* **152**, 48-58

56. Ahmadian, M., Abbott, M. J., Tang, T., Hudak, C. S., Kim, Y., Bruss, M., Hellerstein, M. K., Lee, H. Y., Samuel, V. T., Shulman, G. I., Wang, Y., Duncan, R. E., Kang, C., and Sul, H. S. (2011) Desnutrin/ATGL is regulated by AMPK and is required for a brown adipose phenotype. *Cell Metab* **13**, 739-748

57. Badin, P. M., Langin, D., and Moro, C. (2013) Dynamics of skeletal muscle lipid pools. *Trends Endocrinol Metab* **24**, 607-615

58. Guo, Z., Burguera, B., and Jensen, M. D. (2000) Kinetics of intramuscular triglyceride fatty acids in exercising humans. *J Appl Physiol (1985)* **89**, 2057-2064

59. Kanaley, J. A., Shadid, S., Sheehan, M. T., Guo, Z., and Jensen, M. D. (2009) Relationship between plasma free fatty acid, intramyocellular triglycerides and long-chain acylcarnitines in resting humans. *J Physiol* **587**, 5939-5950

60. Kanaley, J. A., Shadid, S., Sheehan, M. T., Guo, Z., and Jensen, M. D. (2013) Hyperinsulinemia and skeletal muscle fatty acid trafficking. *Am J Physiol Endocrinol Metab* **305**, E540-548

61. Cooper, D. E., Grevengoed, T. J., Klett, E. L., and Coleman, R. A. (2015) Glycerol-3-phosphate Acyltransferase Isoform-4 (GPAT4) Limits Oxidation of Exogenous Fatty Acids in Brown Adipocytes. *J Biol Chem* **290**, 15112-15120

62. Yang, L. Y., Kuksis, A., Myher, J. J., and Steiner, G. (1995) Origin of triacylglycerol moiety of plasma very low density lipoproteins in the rat: structural studies. *J Lipid Res* **36**, 125-136

63. Yang, L. Y., Kuksis, A., Myher, J. J., and Steiner, G. (1996) Contribution of de novo fatty acid synthesis to very low density lipoprotein triacylglycerols: evidence from mass isotopomer distribution analysis of fatty acids synthesized from [2H6]ethanol. *J Lipid Res* **37**, 262-274

64. Lankester, D., Brown, A., and Zammit, V. (1998) Use of cytosolic triacylglycerol hydrolysis products and of exogenous fatty cid for the synthesis of triacylglycerol secreted by cultured hepatocytes. *J. Lipid Res.* **32**, 1635-1645

65. Zammit, V. A., Buckett, L. K., Turnbull, A. V., Wure, H., and Proven, A. (2008) Diacylglycerol acyltransferases: Potential roles as pharmacological targets. *Pharmacol Ther* **118**, 295-302

66. Ong, K. T., Mashek, M. T., Bu, S. Y., Greenberg, A. S., and Mashek, D. G. (2011) Adipose triglyceride lipase is a major hepatic lipase that regulates triacylglycerol turnover and fatty acid signaling and partitioning. *Hepatology* **53**, 116-126

67. Kuerschner, L., Moessinger, C., and Thiele, C. (2008) Imaging of lipid biosynthesis: how a neutral lipid enters lipid droplets. *Traffic* **9**, 338-352

68. Adams, B. A., Gray, S. L., Isaac, E. R., Bianco, A. C., Vidal-Puig, A. J., and Sherwood, N. M. (2008) Feeding and metabolism in mice lacking pituitary adenylate cyclase-activating polypeptide. *Endocrinology* **149**, 1571-1580

LEGENDS TO FIGURES

Figure 1 DGAT1 and DGAT2 mRNA expression in mouse tissues

The levels of mRNA expression of (a) DGAT1 and (b) DGAT2 were measured in the mouse tissues indicated. Values are means (± SEM) for three separate determinations.

Figure 2 Expression of DGAT1, DGAT2 and aP2 during differentiation of IMBAT-1 cells

IMBAT-1 cells were differentiated for 6 days (see Methods section). The fold-activation of DGAT1, DGAT2, and aP2 mRNA expression relative to that at day 0, during subsequent differentiation. The variances of input cDNA were normalised against the levels of three housekeeping genes; L19, B-actin and 36B4. Values are means (±SEM) for three separate determinations for separate cell preparations. Note different scale of y-axis for DGAT2. Where error bars are not shown, they lie within the symbols.

Figure 3 Etomoxir selectively prevents the increase in glucose-derived CO_2 formation after β3-adrenergic stimulation of IMBAT-1 cells, but not the increased incorporation into the glyceryl and acyl moieties of TG

Cells were incubated with CL for 2h, followed by a further incubation period of 2h, at the start of which U-^{14}C-glucose label was added (at zero time) as described in the Methods section. Incorporation of label was measured into (a) CO_2, and (b) glyceryl- and **(c)** acyl-moieties of TG. Etomoxir (Etmox) was added 30 min before the addition of label. Data are means (± SEM) for three separate experiments, and are expressed with respect to paired controls, which are set at 100% for each experiment. Values that were significantly statistically different ($P \leq 0.05$) are indicated by * (*vs* control) or # (CL+Etomoxir *vs* CL).

Figure 4 ATGL inhibition prevents β3-induced stimulation of U-^{14}C-glucose incorporation into TG and CO_2.

Cells were incubated with CL for 2h before addition of U-^{14}C-glucose, and incorporation of label into (a) CO_2 and (b) TG was measured during a further 2h incubation (see Methods). When Atglistatin (Astat) or THL were present, they were added at the same time as CL. Data are means (±SEM) for three separate experiments, and are expressed with respect to Control values which are set at 100% for each experiment. Values that were statistically significantly different ($P<0.05$) are indicated by * (CL vs Control) and # (CL+THL or CL+Astat vs. CL).

Figure 5 Effect of DGAT1 and DGAT2 inhibition on the incorporation of U-^{14}C glucose into CO_2 and TG after β3-agonist stimulation of IMBAT-1 cells.

Cells were incubated with CL for 2h before the start of incubations by the addition of U-^{14}C-glucose label). Inhibitors were added individually 30 min before the addition of label (see Methods section). Experiments were performed in the absence (a–c) or presence (d–f) of oleate (0.75mM with 0.25% BSA) and glycerol (0.75mM). Incorporation of label from U-^{14}C-glucose was measured for a 2h period into CO_2 (a, d), TG-acyl moieties (b, e), and TG-glyceryl moieties (c, f). The concentrations of inhibitors used were: DGAT1-iB, 0.75 μM; DGAT2-iC, 50 μM, and DGAT2-iJ, 50 μM. Values are means (±SEM) for three separate experiments and are expressed with respect to values for Controls (set at 100%) to which no CL or inhibitors were added. Values that were statistical significantly different ($P<0.05$) are indicated by * (CL vs Control) and # (CL + inhibitors vs CL only).

Figure 6 Effects of siRNA-mediated DGAT1- or DGAT2-knockdown on the respective levels of mRNA expression of the two enzymes

Differentiated cells were treated for 72h with either control (scrambled, SC) siRNA or siRNA targeted towards DGAT1 (SiD1) or DGAT2 (SiD2) and the level of (a) DGAT1 and (b) DGAT2 mRNA expression was measured. Values (n=3) are means (±SEM) for a representative experiment. Values that were statistically significantly different ($P<0.05$) from SC are indicated by an asterisk.

Figure 7 Effects of siRNA-mediated DGAT1- or DGAT2-knockdown on the rates of incorporation of U-^{14}C-glucose into CO_2 and TG in the presence or absence of β3-adrenergic stimulation of IMBAT-1 cells.

Differentiated cells were treated for 72h with either control (scrambled, SC) siRNA or siRNA (SiD) targeted towards DGAT1 (SiD1) or DGAT2 (SiD2) - see Methods section. Cells were incubated +/- CL for 2h, followed by the measurement of the incorporation of label from U-^{14}C-glucose into (a) CO_2, (b) total TG, and (c,e) TG-glyceryl and (d,f) TG-acyl moieties of TG. Data are means (±SEM) for three separate experiments and are expressed with respect to Control values (which are set at 100%) for each experiment. Values that are statistically significantly different ($P<0.05$) are indicated by * (SC+CL or SiD *vs* SC) and # (SiD+CL *vs* SC+CL).

Figure 8 Effect of siRNA-mediated knockdown of DGAT1 and DGAT2 on the expression of genes involved in pathways leading from glucose to TG-synthesis and CO_2 formation

Differentiated cells were treated for 72h with control siRNA (scrambled, SC) or siRNA targeted against DGAT1 (SiD1) or DGAT2 (SiD2). mRNA determinations were performed on cells incubated for 2h either in the absence (-) or presence (+) of CL. The variances of input cDNA were normalised against the levels of three housekeeping genes; L19, B-actin and 36B4, and expressed relative to those of SC, which were set at 1.0. Values are means (±SEM) for three separate experiments. Values that were statistically significantly different ($P<0.05$) are indicated by * (*vs* SC) and # (*vs* SC+CL). ACC1, acetyl-CoA carboxylase 1; FASN, fatty acid synthase.

Figure 9 Effects of individual or combined inhibition of DGAT1 and DGAT2 on the incorporation of added oleate or glycerol into TG

Cells were incubated with glucose, oleate and glycerol (see text for concentrations). When present, CL was added 2h before the addition of label, either (a) 1-^{14}C-oleate or (b) 2-^{3}H-glycerol. The inhibitors (*DGAT1-iB* to inhibit DGAT1, and *DGAT2-iJ*, to inhibit DGAT2 specifically) were added 30 min before the addition of label. Values

are means (±SEM) for three separate experiments. Values that are statistically significantly different from those for Control ($P<0.05$) are indicated by an asterisk.

Figure 10 Effect of DGAT1 and DGAT2 inhibition on the incorporation of U-^{14}C glucose into CO_2 and TG after β3-agonist stimulation of primary brown adipocytes

Cells were incubated with CL for 2h before the start of incubations by the addition of U-^{14}C-glucose label). Inhibitors were added individually 30 min before the addition of label (see Methods section). Experiments were performed in presence of oleate (0.75mM with 0.25% BSA) and glycerol (0.75mM). Incorporation of label from U-^{14}C-glucose was measured for a 2h period into (a) TG-glyceryl moieties, (b) TG-acyl moieties and (c) CO_2. The concentrations of inhibitors used were: DGAT1-iB, 0.75 μM; DGAT2-iC, 50 μM, and DGAT2-iJ, 50 μM. Values are means (±SEM) for three separate experiments and are expressed with respect to values for Controls (set at 100%) to which no CL or inhibitors were added. Values that were statistical significantly different ($P<0.05$) are indicated by * (CL vs Control) and # (CL + inhibitors vs CL only).

Figure 11 Proposed pathways that link DGAT2 to *de novo* fatty acid synthesis and thermogenesis in brown adipocytes

Fatty acids synthesised *de novo* from glucose (FA'') are used to form a pool of diglyceride (DG'') which is esterified with FA'' by DGAT2 to form a distinct pool of triglyceride (TG''). Adrenergic (β3) stimulation simultaneously activates *de novo* lipogenesis and TG lipolysis. A product of lipolysis activates the process of glucose utilization for lipogenesis (DNL) upon stimulation of the cells by β3-agonists through a positive feedback mechanism which is interrupted by inhibition of ATGL. TG lipolysis provides FA substrate for uncoupled mitochondrial oxidation. FA activate UCP1, the expression of which is increased by β3-action. Glycerol-3-P synthesised from exogenous glycerol is used for the synthesis of a separate DG pool (DG') which is used as a substrate for re/esterification preferentially by DGAT1, and to a lesser extent by DGAT2. Glycerol-3-P generated endogenously from glucose is used to form both DG'' and DG'. Exogenous FA is not oxidised directly, but is re/esterified by DGAT1 or DGAT2 redundantly into/within a larger TG pool (TG') before oxidation.

Figure 1

(a)

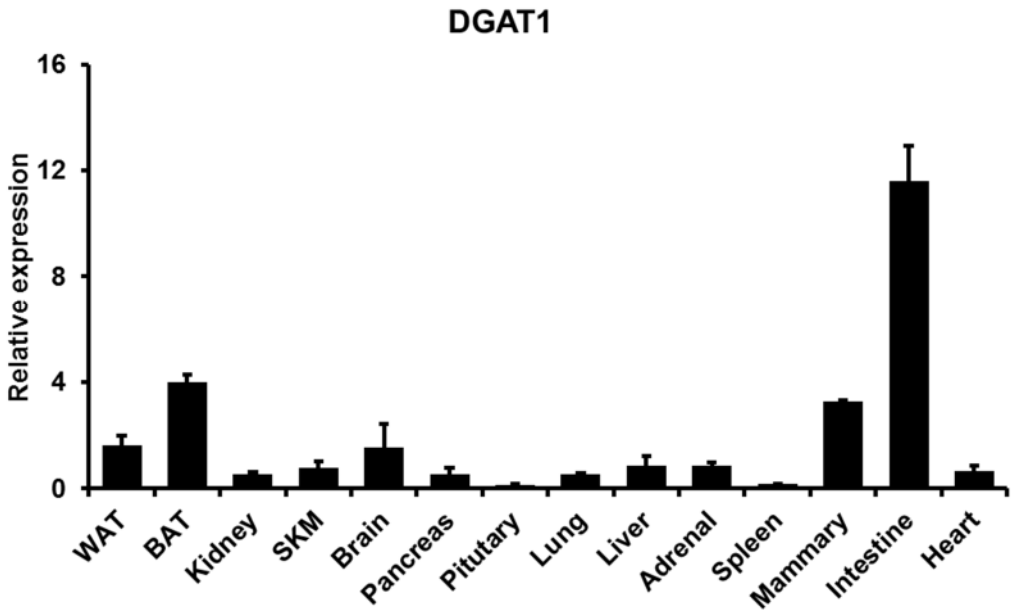
DGAT1
Relative expression
16
12
8
4
0
WAT
BAT
Kidney
SKM
Brain
Pancreas
Pitutary
Lung
Liver
Adrenal
Spleen
Mammary
Intestine
Heart

(b)

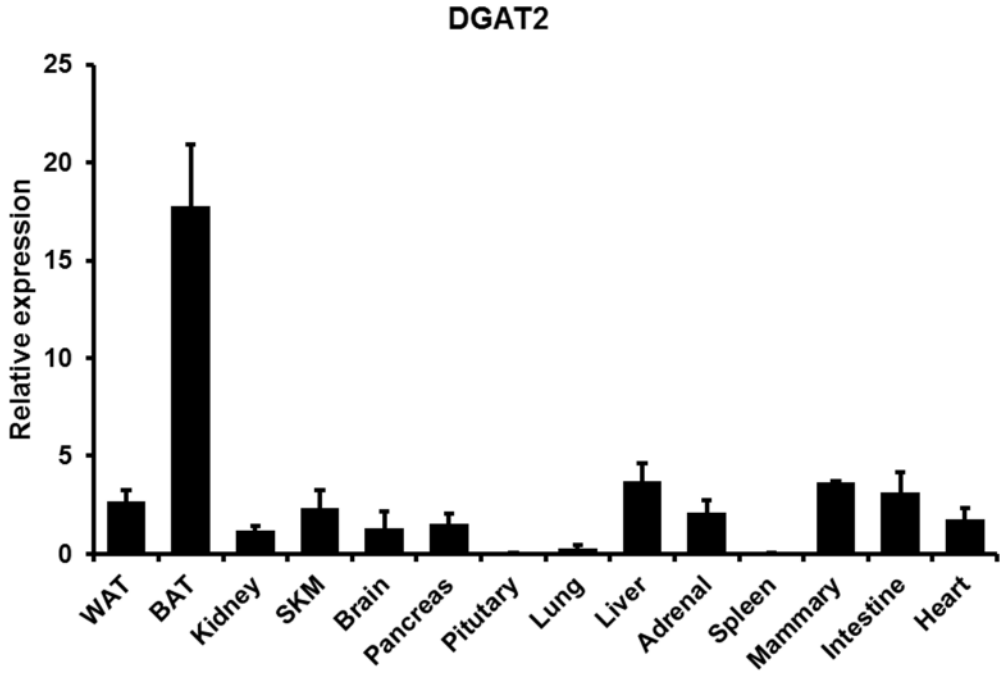
DGAT2
Relative expression
25
20
15
10
5
0
WAT
BAT
Kidney
SKM
Brain
Pancreas
Pitutary
Lung
Liver
Adrenal
Spleen
Mammary
Intestine
Heart

Figure 2

(a)

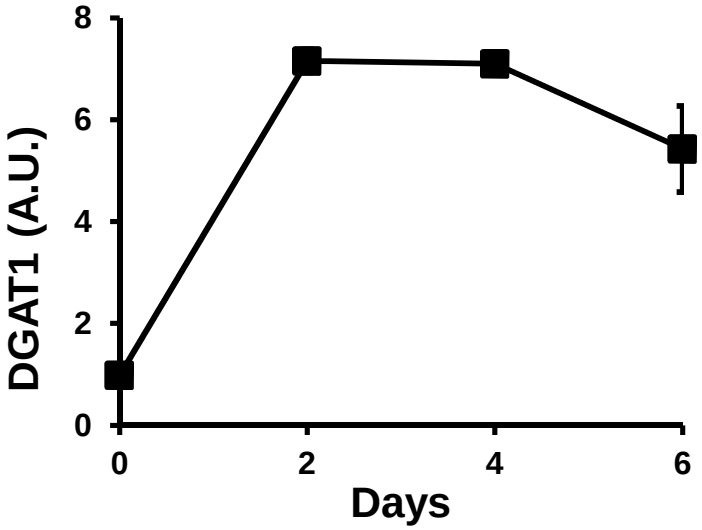
DGAT1 (A.U.)
0
2
4
6
8
0
2
4
6
Days

(b)

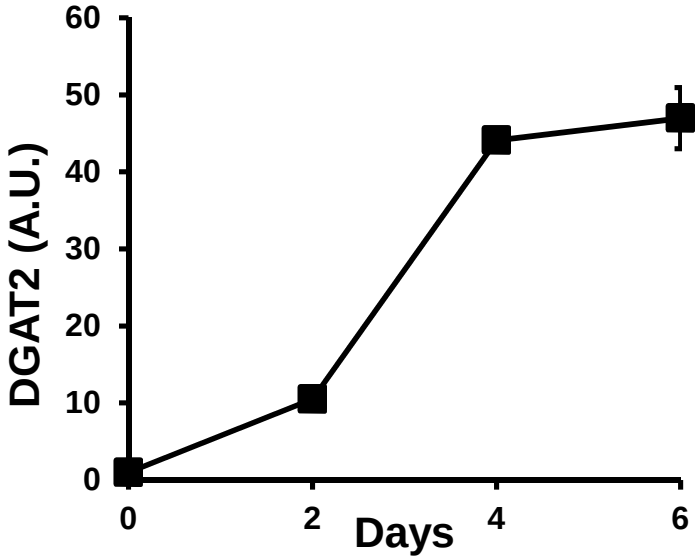
DGAT2 (A.U.)
0
10
20
30
40
50
60
0
2
4
6
Days

(c)

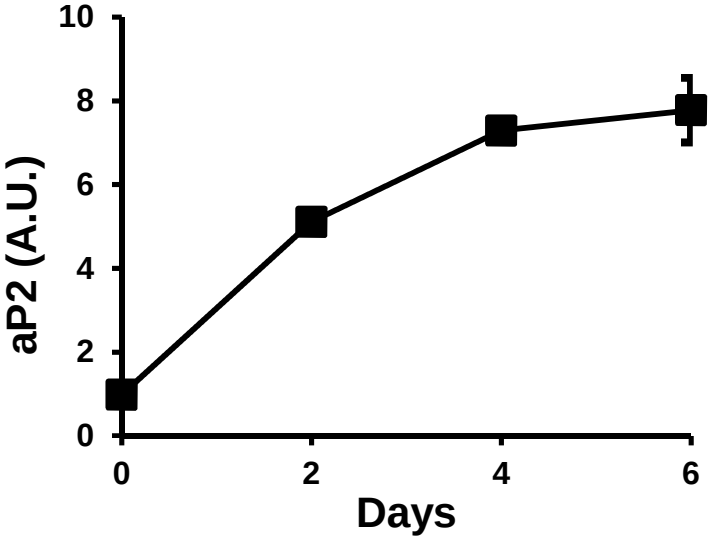
aP2 (A.U.)
0
2
4
6
8
10
0
2
4
6
Days

Figure 3

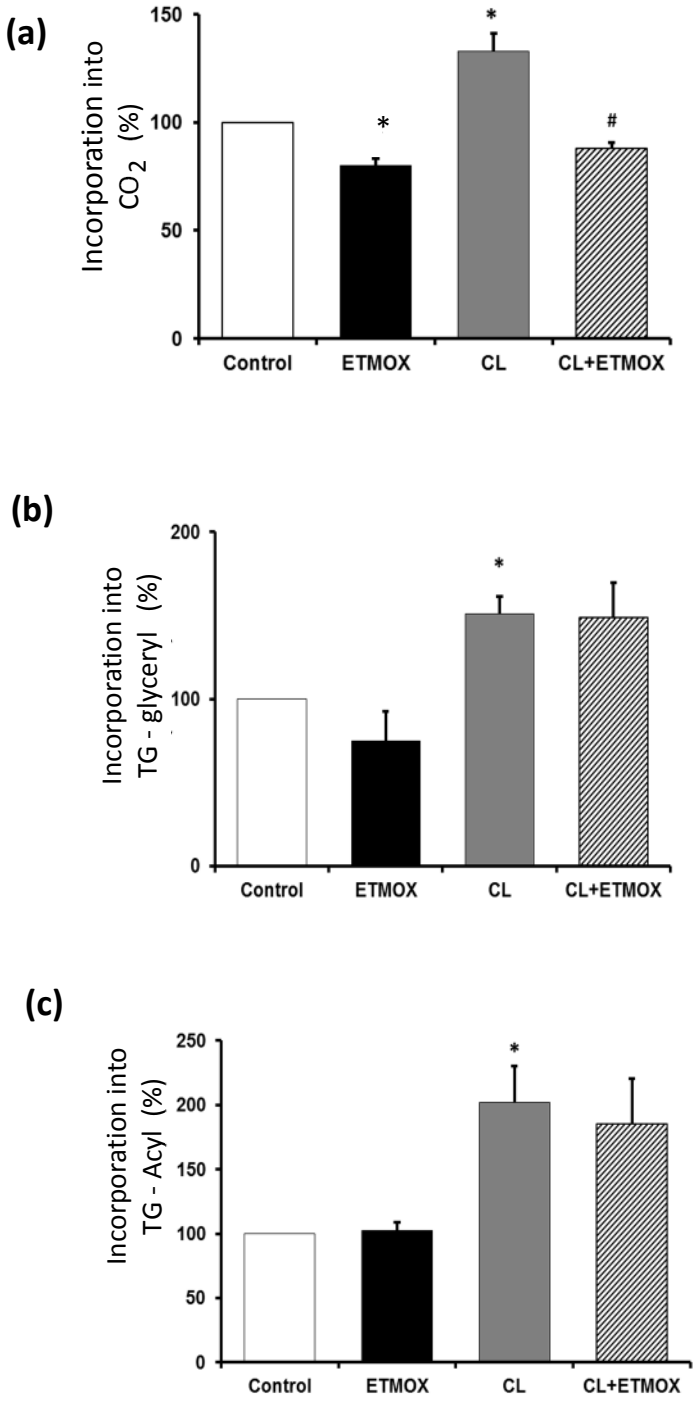
(a)
Incorporation into CO_2 (%)
150
100
50
0
*
*
#
Control
ETMOX
CL
CL+ETMOX
(b)
Incorporation into TG - glyceryl (%)
200
100
0
*
Control
ETMOX
CL
CL+ETMOX
(c)
Incorporation into TG - Acyl (%)
250
200
150
100
50
0
*
Control
ETMOX
CL
CL+ETMOX

Figure 4

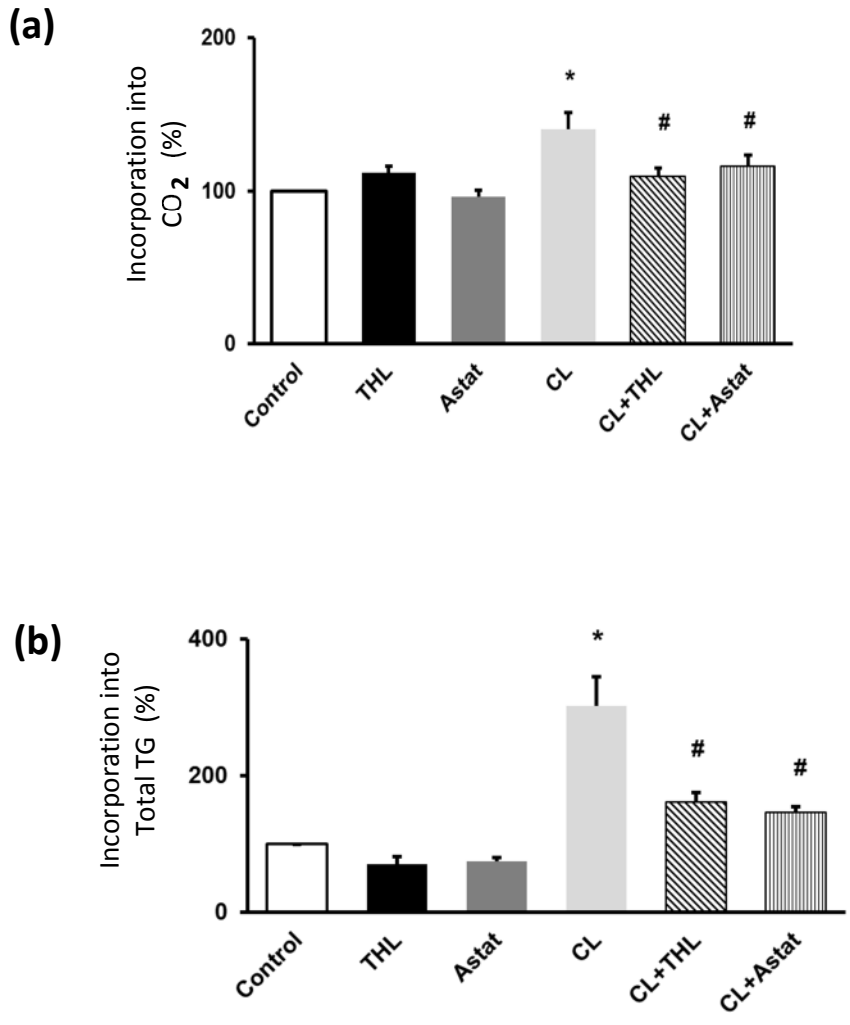
(a)
Incorporation into CO_2 (%)
200
100
0
*
#
#
Control
THL
Astat
CL
CL+THL
CL+Astat
(b)
Incorporation into Total TG (%)
400
200
0
*
#
#
Control
THL
Astat
CL
CL+THL
CL+Astat

Figure 5

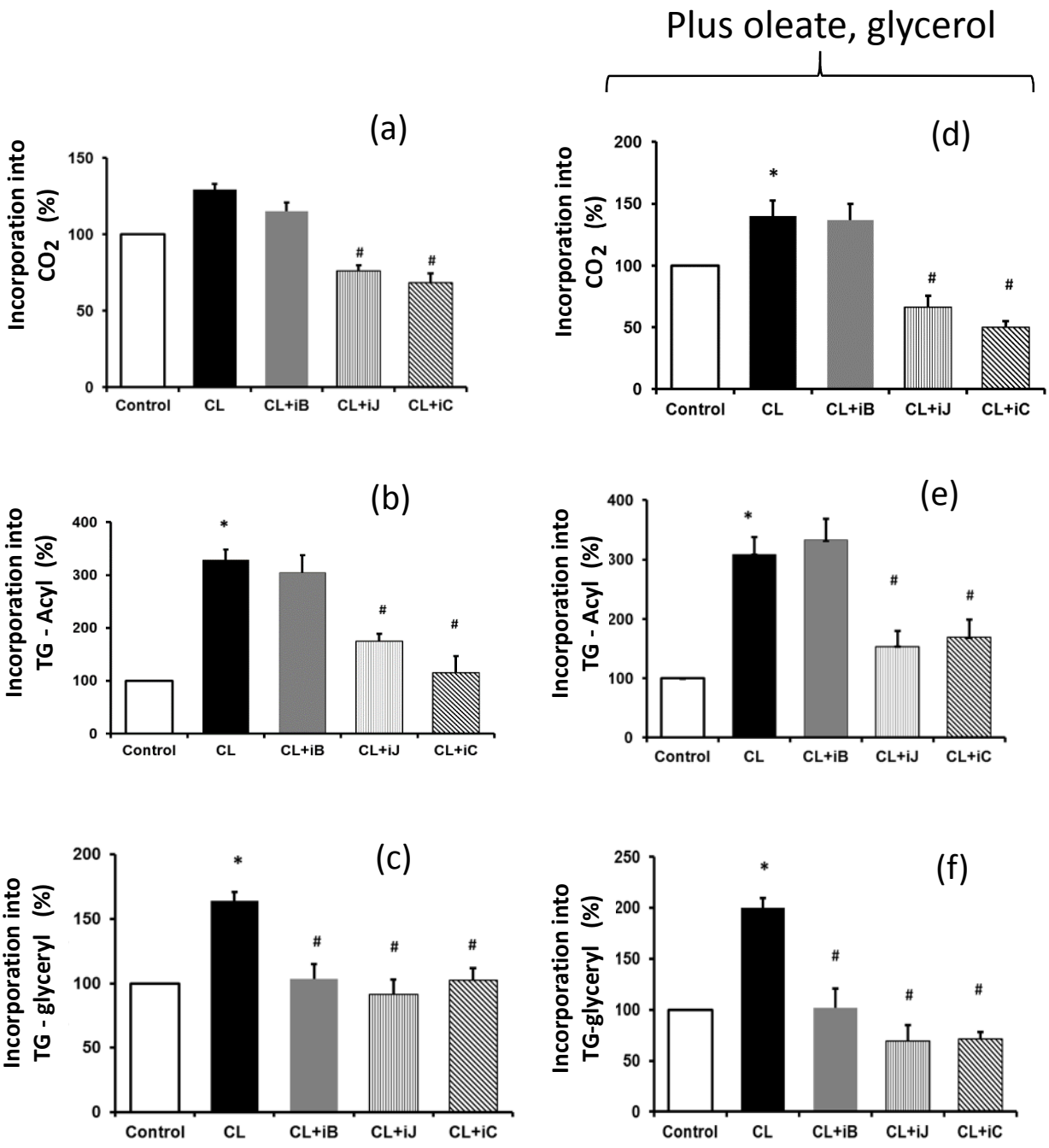
Plus oleate, glycerol
(a)
(b)
(c)
(d)
(e)
(f)
Incorporation into CO_2 (%)
Incorporation into TG - Acyl (%)
Incorporation into TG - glyceryl (%)
Incorporation into TG-glyceryl (%)
Control
CL
CL+iB
CL+iJ
CL+iC
*
#

Figure 6

(a)

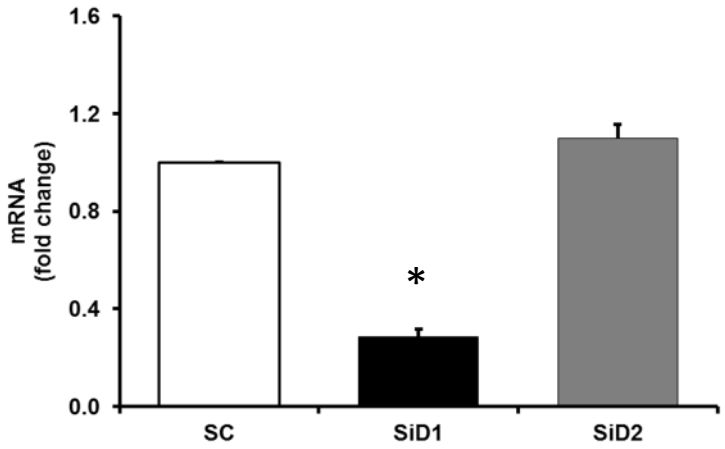
DGAT1
mRNA (fold change)
1.6
1.2
0.8
0.4
0.0
*
SC
SiD1
SiD2

(b)

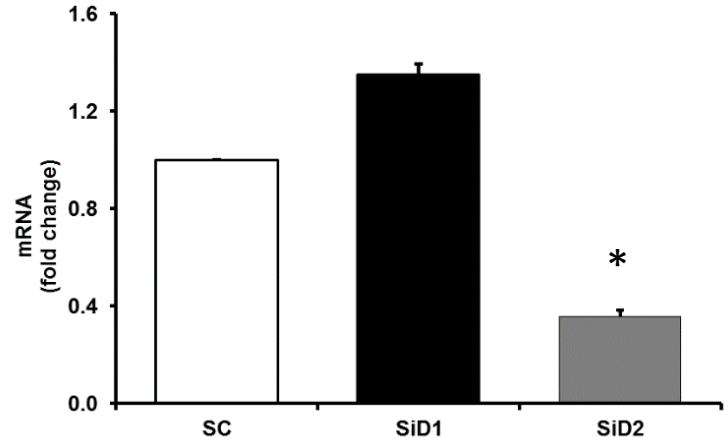
DGAT2
mRNA (fold change)
1.6
1.2
0.8
0.4
0.0
*
SC
SiD1
SiD2

Figure 7

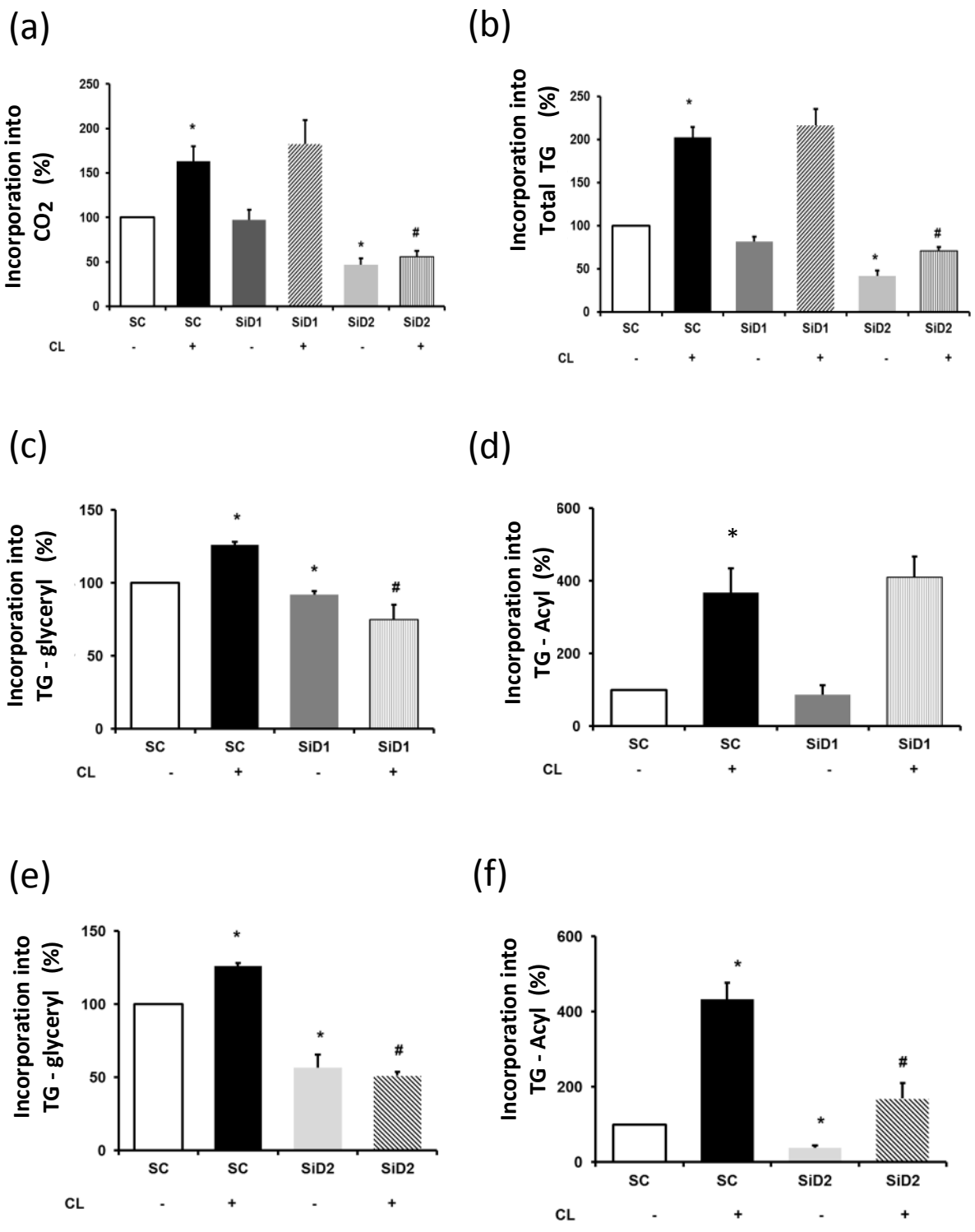
(a)
Incorporation into CO2 (%)
250
200
150
100
50
0
*
*
#
SC
SC
SiD1
SiD1
SiD2
SiD2
CL
-
+
-
+
-
+
(b)
Incorporation into Total TG (%)
250
200
150
100
50
0
*
*
#
SC
SC
SiD1
SiD1
SiD2
SiD2
CL
-
+
-
+
-
+
(c)
Incorporation into TG - glyceryl (%)
150
100
50
0
*
*
#
SC
SC
SiD1
SiD1
CL
-
+
-
+
(d)
Incorporation into TG - Acyl (%)
600
400
200
0
*
SC
SC
SiD1
SiD1
CL
-
+
-
+
(e)
Incorporation into TG - glyceryl (%)
150
100
50
0
*
*
#
SC
SC
SiD2
SiD2
CL
-
+
-
+
(f)
Incorporation into TG - Acyl (%)
600
400
200
0
*
*
#
SC
SC
SiD2
SiD2
CL
-
+
-
+

Fig 8

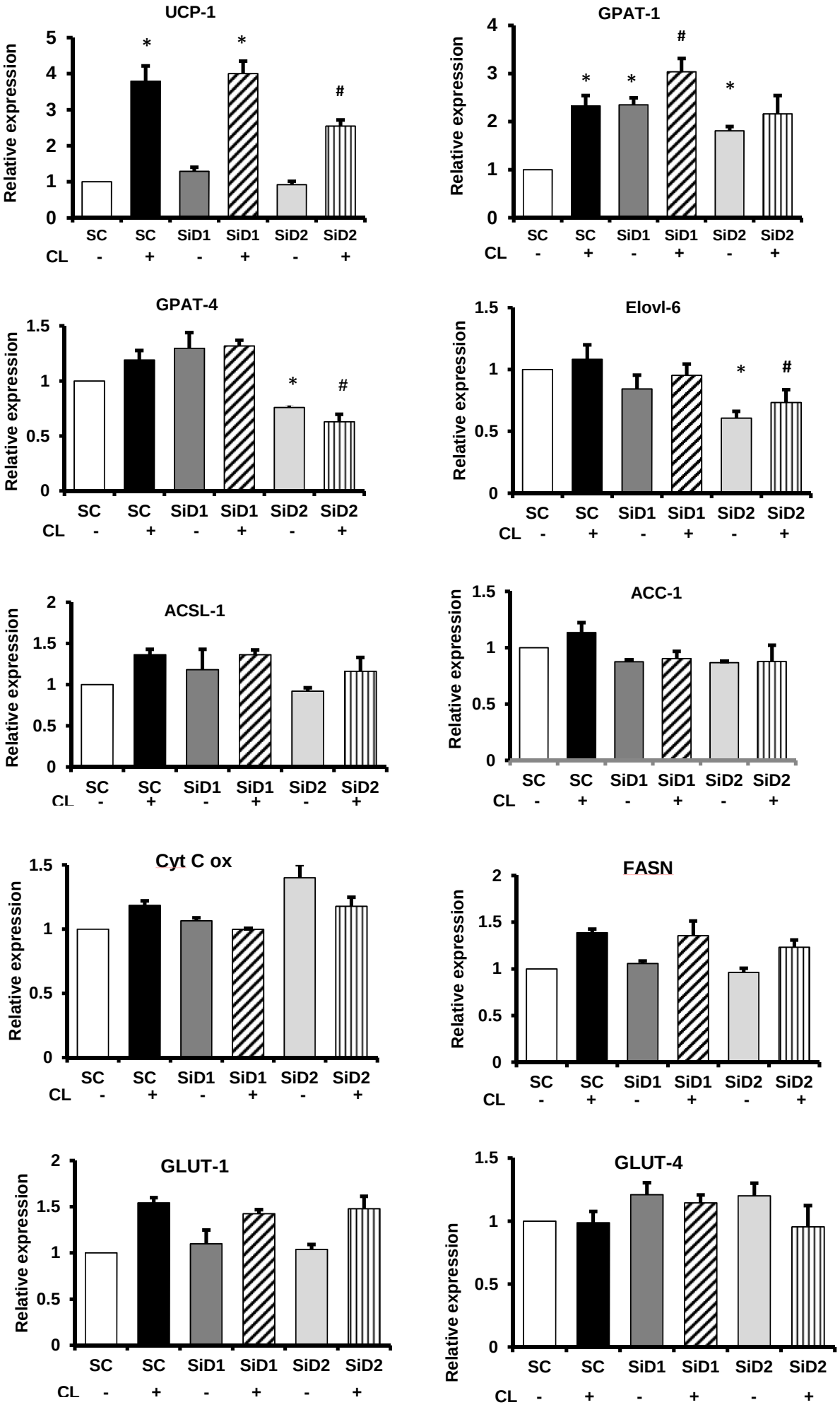
UCP-1
GPAT-1
GPAT-4
Elovl-6
ACSL-1
ACC-1
Cyt C ox
FASN
GLUT-1
GLUT-4
Relative expression
SC SC SiD1 SiD1 SiD2 SiD2
CL - + - + - +

Figure 9

(a)

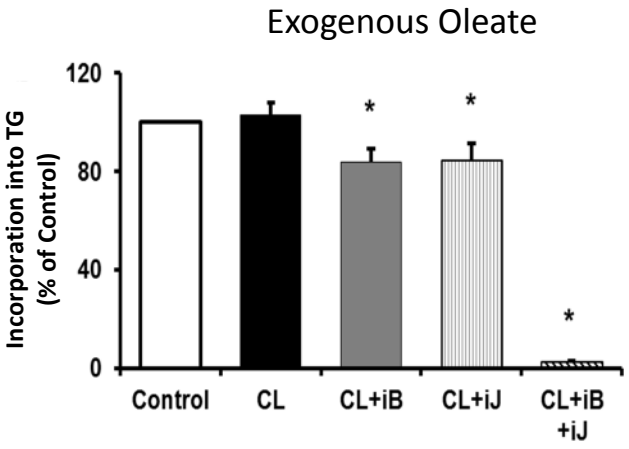
Exogenous Oleate
Incorporation into TG (% of Control)
120
80
40
0
*
*
*
Control
CL
CL+iB
CL+iJ
CL+iB +iJ

(b)

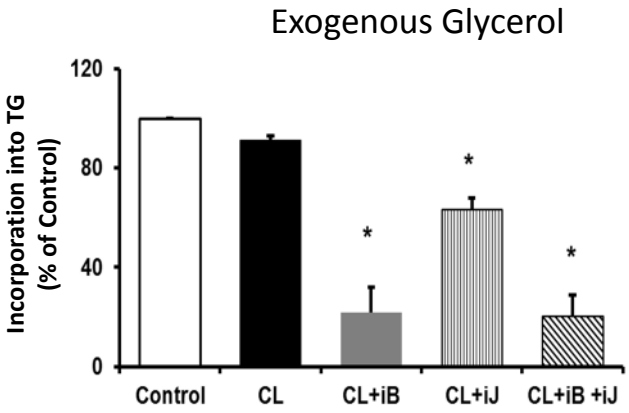
Exogenous Glycerol
Incorporation into TG (% of Control)
120
80
40
0
*
*
*
Control
CL
CL+iB
CL+iJ
CL+iB +iJ

Figure 10

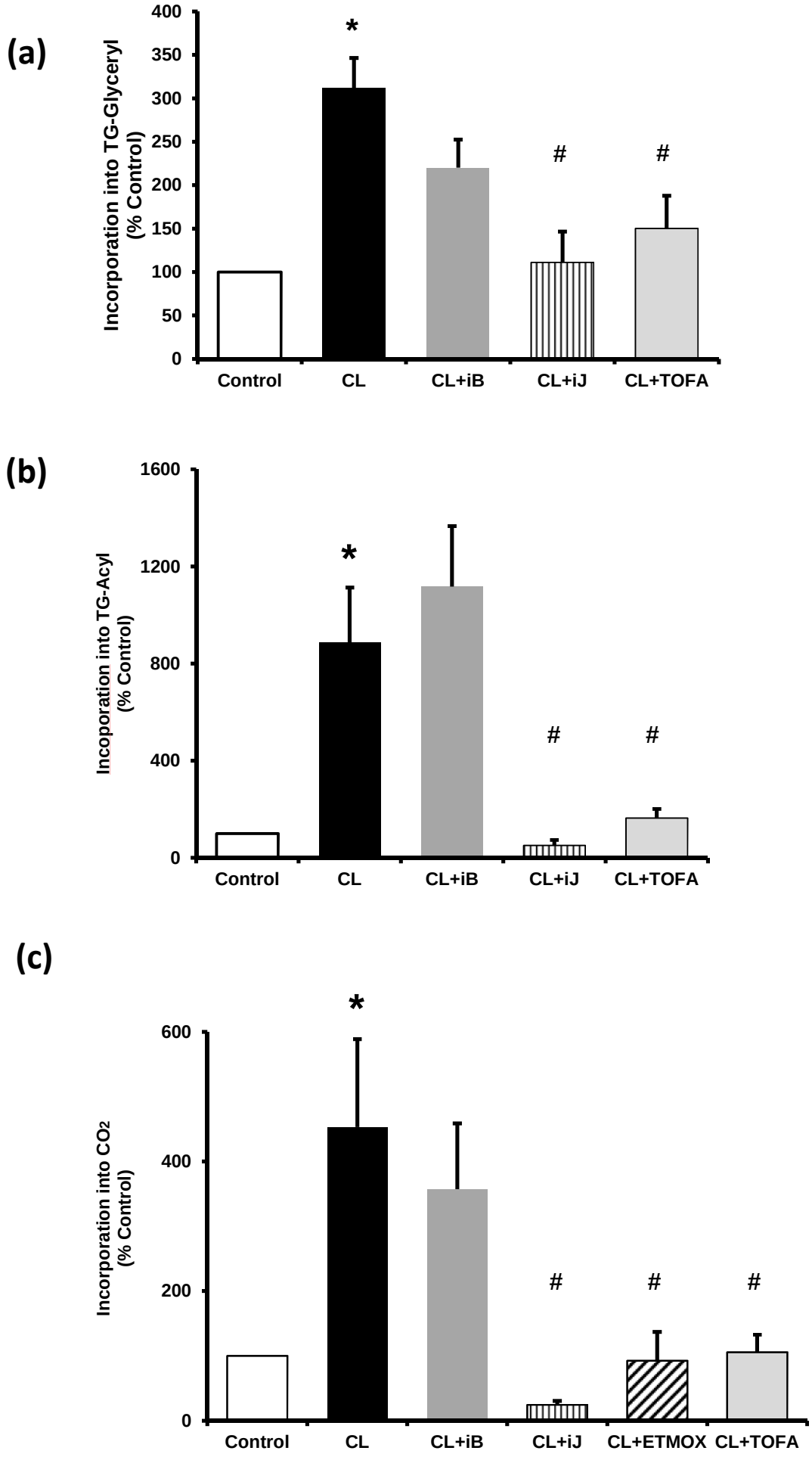
(a)
Incorporation into TG-Glyceryl (% Control)
400
350
300
250
200
150
100
50
0
*
#
#
Control
CL
CL+iB
CL+iJ
CL+TOFA
(b)
Incoporation into TG-Acyl (% Control)
1600
1200
800
400
0
*
#
#
Control
CL
CL+iB
CL+iJ
CL+TOFA
(c)
Incorporation into CO2 (% Control)
600
400
200
0
*
#
#
#
Control
CL
CL+iB
CL+iJ
CL+ETMOX
CL+TOFA

Figure 11

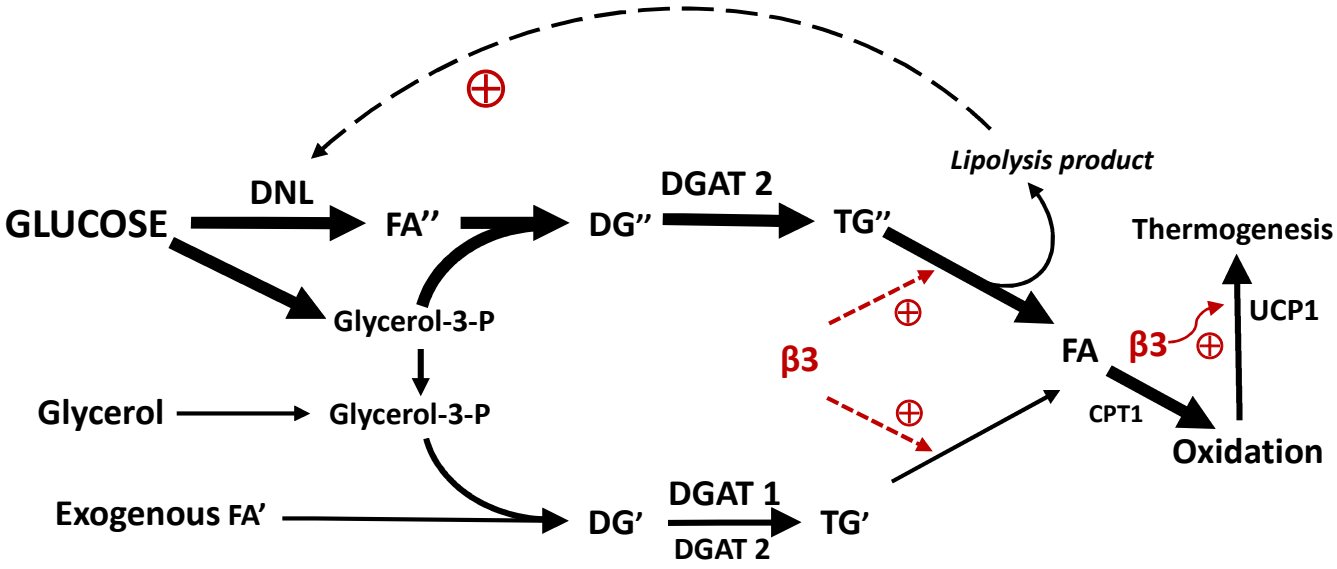
GLUCOSE
DNL
FA''
DG''
DGAT 2
TG''
Lipolysis product
Thermogenesis
UCP1
Glycerol-3-P
β3
FA
β3
Glycerol
Glycerol-3-P
CPT1
Oxidation
Exogenous FA'
DG'
DGAT 1
DGAT 2
TG'